ington, MA), and antibiotics. The cells were then placed in a humidified, 5% CO_2/95% air incubator at 37°C and the medium was subsequently changed every other day. From day 4 (96 hours after plating), 1% dimethyl sulfoxide (DMSO; Aldrich Chemical Co., Inc., Milwaukee, WI) was added to the culture medium and cells were cultured for 12 days.

Cultured SHs at day 12 were dissociated with solution (Cell Dissociation Solution; Sigma Chemical Co.) for 5 minutes after pretreatment with 0.02% EDTA/PBS for 1 minute. Two × 10^6 (cells/ml) viable SHs were resuspended with saline and used for HT.

Hepatic Irradiation

Hepatic irradiation was performed under open laparotomy. The recipient rats were placed in the supine position on a cork platform. Anesthesia was induced by intraperitoneal injection of 12.5 mg/ml/kg pentobarbital sodium (Dainippon Pharmaceutical Co., Osaka, Japan). Two-by-three centimeter lead shields were wedged under the liver to protect other organs. A Softex X-ray irradiation device (M-150WE; Softex, Kanagawa, Japan) was used (120 kVp, 6 mA, 437 mm SSD, dose rate 3.32 Gy/min). The dose delivered to the liver was verified by dosimetry with an exclusive probe into the abdominal cavity.

Hepatocyte Transplantation

Forty-eight hours after hepatic irradiation, intrasplenic HT was performed. Female DPPIV- F344 rats and NAR rats were anesthetized with ether inhalation and the lower pole of the spleen was exposed by a left flank incision. Then 0.5 ml of saline (control group), male primary FHs (2 × 10^7 cells/0.5 ml) or male cultured SHs (1 × 10^6 cells/0.5 ml) were injected into the splenic pulp of the female rats. The hole for the injection was tied with 4-0 silk to achieve hemostasis.

Immunosupressive Treatment

The recipient female NAR rats in all the groups received 10 mg/kg cyclosporine (Calbiochem, La Jolla, CA) to suppress immune rejection of allogenic donor cells, and 2 mg/kg tetracycline (Sigma Chemical Co.) to prevent opportunistic infection from daily subcutaneous injections.

Experimental Protocol

DPPIV Rat Experiment

The rats were divided into three groups (nine rats for the control group, 18 rats for the FH group, and 18 rats for the SH group). The animals were killed at 1, 4, and 12 weeks after either injection or cell transplantation. In the experimental groups, six rats were killed at each time point and samples were collected for DPPIV enzyme histochemistry and Sry PCR analysis.

NAR Rat Experiment

The rats were divided into three groups (five rats for the control group, six rats for the FH group, and six rats for the SH group). During the experiment, the blood was collected through the jugular vein at 1, 4, 8, and 12 weeks after either saline injection or cell transplantation to measure the serum albumin level. All animals were killed at 12 weeks and samples were collected to examine immunofluorescent histochemistry, albumin mRNA expression by RT-PCR, albumin protein by Western blot analysis, and for Sry PCR analysis.

SH Proliferative Activity

The proliferative activity in cultured SHs before transplantation was determined by measuring incorporation of 5-bromo-2'-deoxyuridine (BrdU), as described previously.[7] Briefly, 40 μM of BrdU was added to each 35 mm dish 24 hours before fixation of cells in cold absolute ethanol. A mouse anti-BrdU antibody (DAKO A/S, Copenhagen, Denmark) was used as the primary antibody. Labeled nuclei in the cells were counted in 20 fields/dish and three different dishes were examined. Data are presented as means ± SD from three independent experiments.

Enzyme Histochemistry for Dipeptidyl Peptidase IV

DPPIV enzyme activity was detected as previously described.[18] Briefly, 8 μm liver and spleen cryosections were fixed in cold acetone for 10 min and air-dried. The samples were incubated for 60 minutes in a substrate solution containing 0.5 mg/mL gly-pro-methoxy-β-naphthylamide (Sigma Chemical Co.), 1.0 mg/mL Fast Blue BB (Sigma Chemical Co.), 100 mmol/L phosphate-buffer (pH 6.5), and 100 mmol/L NaCl. All tissue sections were counterstained with hematoxylin and mounted in glycerol.

Confocal Laser Scanning Microscopic Analysis for CK8 and Albumin

Engrafted hepatocytes were detected by CK8 and albumin double immunofluorescence. Then 8 μm liver and spleen cryosections were fixed in 4% paraformaldehyde for 10 minutes. The samples were incubated for 60 minutes at 4°C with rabbit anti-rat albumin IgG (Cappel, Durham, NC) and monoclonal anti-cytokeratin-8 IgG (Amersham Biosciences Corp., NJ) as the primary antibodies after blocking with normal goat serum. The samples were washed twice with PBS and incubated with Alexa^{488}-conjugated anti-rabbit IgG (Molecular Probes, Eugene, OR) and Alexa^{594}-conjugated anti-mouse IgG (Molecular Probes) as the secondary antibodies. A confocal laser scanning microscope (MRC-1024ES; Bio-Rad Laboratories, Inc., Hercules, CA) was used to detect the signals.

Measurement of Serum Albumin Level

The sera collected in NAR rat experiments were sent to a commercial laboratory (SRL, Inc., Tokyo, Japan) for albumin analysis. The albumin levels were determined by the BCG method using an automated clinical microchemistry system (OLYMPUS AU-5400; Olympus Optical Co.) with its exclusive reagent (Alb-HR2; Wako Pure Chem.).

Polymerase Chain Reaction (PCR) and RT-PCR

For DNA analysis, genomic DNA from the liver and spleen was extracted using a GenElute Mammalian Genomic DNA kit (Sigma Chemical Co.). PCR for the rat *Sry* gene was performed using *Sry* primers (sense 5'-CAGAGATCAGCAAGCATCTGG-3'; anti-sense 5'-TCTGGTTCTTGGAGGACTGG-3')[16] at 94°C for 30 seconds, 57°C for 30 seconds, and 72°C for 30 seconds with 28 cycles. Percentages of engrafted cells were calculated by dilution analyses of hepatocyte DNA between male and/or female cells. *Sry* DPPIV$^+$ male rat hepatocytes were serially diluted with DPPIV$^-$ female rat hepatocytes.

For RNA analysis, tRNA was extracted from the liver and spleen using TRIzol Reagent (Invitrogen Co., Carlsbad, CA). Reverse transcription was performed using an Omniscript Reverse Transcription kit (QIAGEN, Valencia, CA). PCR reaction was performed using *Albumin* primers (sense 5'-GACAAGTTATGCGCCATTCC-3'; anti-sense 5'-ACTGGGTCAGAACCTCATTG-3')[19] at 94°C for 30 sec, 60°C for 30 sec, and 72°C for 30 sec with 26 cycles. Rat *G3PDH* was used as a control (sense 5'-ACCACAGTCCATGCCATCAC-3'; anti-sense 5'-TCCACCACCCTGTTGCTGTA-3') (Clontech Laboratories, Inc., Palo Alto, CA) at 94°C for 30 seconds, 57°C for 30 seconds, and 72°C for 1 minute with 26 cycles. A TaKaRa Taq PCR Kit (TAKARA BIO Inc., Shiga, Japan) was used for all PCR reactions.

Western Blot Analysis

The samples were homogenized using a Polytron (Kinematica, Switzerland) with a buffer containing 10 mM Tris-HCl, pH 7.4, 0.1% sodium deoxycholate, 0.1% sodium dodecyl sulfate (SDS), 0.15 M NaCl, 1 mM EDTA, 1% Triton X-100, 0.1 mM phenylmethane sulfonyl fluoride, and 1% Nonidet P-40 to extract protein. A BCA Protein Assay Reagent Kit (Pierce Biotechnology, Inc., Rockford, IL) was used to determine the concentrations. The proteins (20 μg/lane) were separated by SDS-10% polyacrylamide gel electrophoresis and then transferred electrophoretically to a nylon membrane (Immobilon-P; Millipore Corp., Bedford, MA) with a semi-dry transfer cell (Bio-Rad Laboratories, Richmond, CA). A rabbit anti-albumin antibody (Cappel) was used. A horseradish peroxidase-conjugated anti-rabbit IgG antibody (DAKO) was applied and positive bands were detected by incubation in an ECL Western Blotting Detection System (Amersham, Arlington Heights, IL).

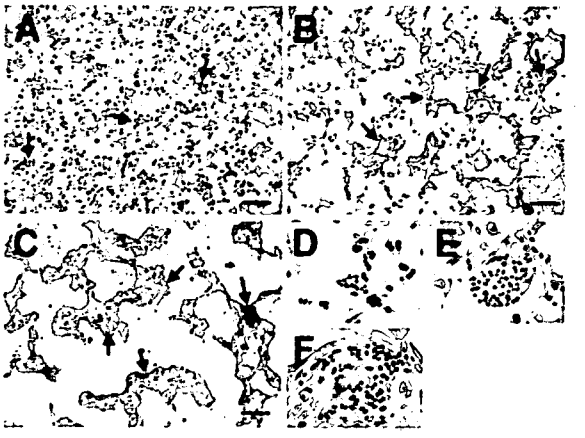

Figure 1. Immunocytochemistry of 5-bromo-2'-deoxyuridine (BrdU) for cultured small hepatocyte colonies at 4 days (A,D), 8 days (B,E), and 12 days (C,F) before hepatocyte transplantation. The cells were labeled with BrdU for 24 hours before harvesting. Arrows indicated the small hepatocyte colonies. The scale bar represents 200 μm.

Densitometric Analysis

Scanning densitometric analysis was performed as previously described.[7] The signals were quantified using the NIH Image 1.55 Densitometric Analysis Program.[20]

Statistical Analysis

Statistical analysis was performed using the StatView 4.5 software package (Abacus Concepts, Inc., Berkeley, CA). All data are expressed as mean ± standard deviation. Statistical significance in each experiment was calculated by either one-way analysis of variance (ANOVA) or Student's unpaired *t*-test when appropriate. A *P*-value < 0.05 was considered significant.

RESULTS

Character of SHs Before Transplantation

We isolated and cultured SHs for 12 days to activate the SH population. SHs could be identified after 4 to 6 days (Fig. 1A,D) in culture. SHs formed colonies and were well identified at day 8 (Fig. 1B,E) and day 12 (Fig. 1C,F). The numbers of SH colonies (Table 1) were 3.83 ± 1.47 (/6.25 mm^2) at day 8 and 4.03 ± 0.86 (/6.25 mm^2) at day 12. The number of SHs per colony increased with time in culture to 17.33 ± 5.92 at day 8 and 26.75 ± 17.31 at day 12, whereas the labeling index in SH colonies significantly decreased from 86.37 ± 8.74 at day 8 to 53.89 ± 5.18 at day 12 ($P < 0.01$). The estimated number of SHs used for HT was calculated to be about 1.0×10^6 (cells/animal), which was less than that of FHs used for HT (about 2.0×10^7 cells/animal).

Hepatocyte Engraftment in Liver and Spleen in the DPPIV Experiment

We used a semi-quantitative method for detection of engrafted cells in the recipients. Fragments of the Y-

chromosome were amplified and compared to control DNA from the mixture of male and female cells (Fig. 2A). In the liver, signals of the Y-chromosome in both groups increased with time in the experiment and the pattern of the increment was similar, although the average level of the signals in the FH group was greater than that in the SH group (Fig. 2B). On the other hand, in the spleen, the signals in both groups decreased with time in the experiments. The signals in the FH group decreased much more rapidly than in the SH group (Fig. 2C). Therefore, the signals of the groups were significantly different after 4 weeks.

Morphological Investigation in the DPPIV Rat Experiment

We confirmed cell engraftment by DPPIV enzyme staining. The engrafted cells were seen within the periportal region of the liver and formed island-like structures in both groups. Cell numbers expanded during the experiment. There was no morphological difference between the FH group (Fig. 3A-C) and the SH group (Fig. 3E-G).

TABLE 1. Characteristics of Small Hepatocyte Colonies at 8 And 12 Days Before Hepatocyte Transplantation

Days after plating	8 days	12 days
Number of SH colonies (/6.25 mm2)	3.83 ± 1.47	4.03 ± 0.86
Number of SHs (/colony)	17.33 ± 5.92	26.75 ± 17.31
BrdU Labeling Indices in SH colonies (%)	86.37 ± 8.74	53.89 ± 5.18*

The number of the colonies and small hepatocytes in the colonies were counted in 10 different independent fields from 3 different dishes.
Data shows means ± standard deviations.
*$p < 0.01$.

Two of the six rats in the FH group showed near total replacement of the liver. The engrafted cells aligned with the hepatic cord from the periportal region to the central vein region at 12 weeks after HT (Fig. 3D).

We also observed cell engraftment in the spleen. The cells in the FH group (Fig. 3H-O) were integrated in the liver parenchyma scatteringly; on the other hand, those in the SH group (Fig. 3L-N,P,Q) formed a mass. Moreover, engrafted cells in the SH group showed a hepatic organoid structure (Fig. 3P) and bile ductal structure (Fig. 3Q). The numbers of cells in both groups decreased with time in the experiment. However, massive cell engraftment in the spleen was observed in two of the six rats, which also showed near total hepatic repopulation (Fig. 3K).

Comparison of FHs and SHs as Cell Sources in the NAR Model

We observed much more hepatic cell engraftment in the FH group than in the SH group. On the other hand, there was much more splenic cell engraftment in the SH group than in the FH group without immunosuppression in a previous study. We therefore investigated albumin support in the NAR rat experiment with immunosuppression, which could be similar to the clinical situation of HT.

We measured serum albumin levels in the FH and SH groups periodically. Serum albumin levels in both groups increased with time in the experiment and there was no significant difference between the groups (Fig. 4).

Hepatocyte Engraftment in Liver and Spleen in the NAR Rat Experiment

We investigated hepatocyte engraftment at 12 weeks after HT in all groups (Fig. 5). In the liver, signals of Y-chromosomes were not significantly different between the groups (Table 2). On the other hand, in the spleen, the level of signals in the SH group was significantly higher than that in the FH group (2.9 ± 0.7 vs. 1.9 ± 0.4: $P = 0.013$).

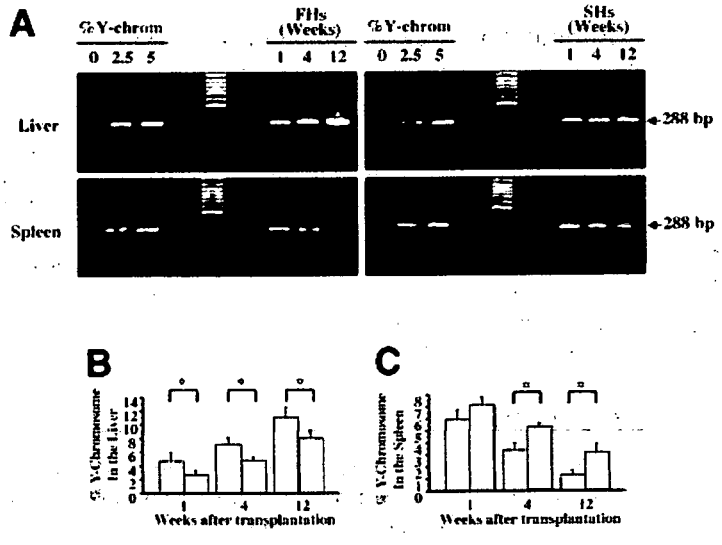

Figure 2. (A) PCR analysis for Y-chromosome gene in recipient organs. The genomic DNA was isolated from 6 different animals at three independent time points. Control amplification of the Y-chromosome was done using a mixture of male and female cells. (B) Densitometric analysis of Y-chromosome gene in the liver. Open columns represent the fresh hepatocyte (FH) group and closed columns represent the small hepatocyte (SH) group. (C) Densitometric analysis of Y-chromosome gene in the spleen. Open columns represent FH group and closed columns represent SH group. Asterisks represent significant differences between the FH group and SH group ($P < 0.05$).

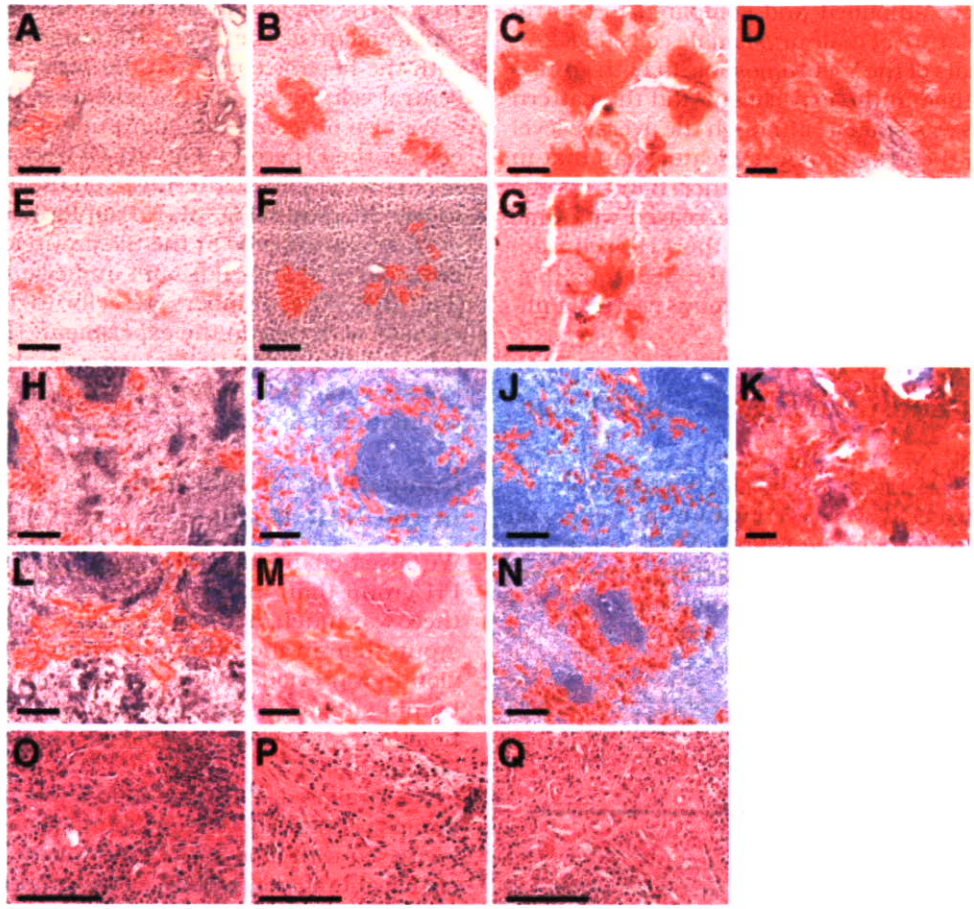

Figure 3. Enzyme histochemistry for dipeptidyl peptidase IV (DPPIV) in the liver (A-G) and in the spleen (H-Q). Hematoxylin-eosin staining of the spleen at 12 weeks in the SH group (O-Q). The specimens were obtained from the FH group (A-D,H-K,O) and SH group (E-G,L-N,P, Q) at 1 week (A,E,H,L), 4 weeks (B,F,I,M), and 12 weeks (C,D,G,J,K,N-Q). The brown staining represents the DPPIV activity. The scale bar represents 100 μm.

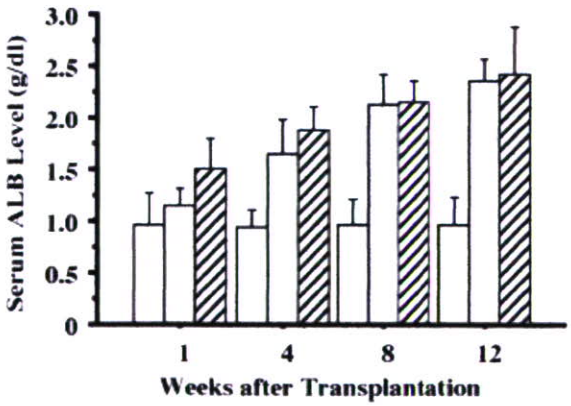

Figure 4. Serum albumin levels in the NAR experiments. Open columns represent the control group, which was injected with saline. Dotted columns represent fresh hepatocyte groups. Shaded columns represent small hepatocyte groups. The bars represent standard deviations.

Albumin mRNA and Protein in the Recipient Organs at 12 Weeks

We found that HT using both FHs and SHs could be effective to improve the serum albumin level in NAR recipients and the cells were detectable at 12 weeks after HT. We observed albumin mRNA expression (Fig. 6A) and protein (Fig. 6B) in the livers and the spleens from six different animals. There was no significant difference in the albumin mRNA expression and protein level between the groups either in the liver or in the spleen (Table 3).

Confocal Laser Scanning Microscopic Analysis of Albumin and CK8

We performed double immunofluorescence analysis of albumin for donor cells and CK8 for hepatocytes, including recipient cells. We detected albumin signals in both groups (Fig. 7). Albumin-positive hepatocytes in the FH group (Fig. 7A) showed a scattered pattern; on the other hand, in SH group (Fig. 7D), they showed colony formation as seen in vitro. All the cells were positive for CK8 (Fig. 7B,E), which is a hepatocyte marker, and all these cells were merged with ALB (Fig. 7C,F).

DISCUSSION

We investigated cell engraftment and the functions of cultured SHs in HT compared to FHs. The donor cell number in the SH group was much smaller than that in

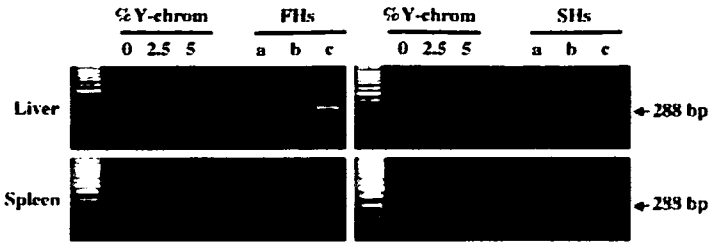

Figure 5. PCR analysis for Y-chromosome gene in female NAR at 12 weeks after hepatocyte transplantation in the fresh hepatocyte (FH) group and small hepatocyte (SH) group. The photographs show three representative data from 6 different animals at 12 weeks. Control amplification of the Y-chromosome was done using a mixture of male and female rat cells.

TABLE 2. Y-chromosome Gene Rate in the Recipient Organs at 12 Weeks After HT

	Y-chromosome (%)		
	FHs	SHs	P value
Liver	7.9 ± 4.4%	4.4 ± 3.4%	NS
Spleen	1.9 ± 0.4%	2.9 ± 0.7%	0.013

All data represent means ± standard deviations.
Organ samples were collected from 6 different animals and intensity of the PCR signals was measured by densitometric analysis as described in Materials and Methods.

the FH group. The cell engraftment in the SH group was smaller in the liver and larger in the spleen than in the FH group in the DPPIV rat experiments. The cell engraftment in the liver increased after HT; however, that in the spleen decreased after HT in both groups. HT using SHs supported the albumin level in the NAR rat experiments as did that using FHs. Thus, long-term cultured SHs could express and support hepatic functions in the repopulating model of the liver.

Potential for SH Proliferation

Although every mature hepatocyte may proliferate after partial hepatectomy,[21] it is uncertain if every one of them can proliferate forever and possess eternal activity. When hepatocytes are cultured for a long term, they do not proliferate equally. This suggests that a limited number of a small population, such as SHs, could exclusively possess high proliferative activity.

We found that the increment of cell engraftment was very similar in the FH and SH groups. This suggested that the 2×10^7 FHs contained similar numbers of cells that could proliferate and repopulate after HT compared to the 1×10^6 SHs. If the SH colony was generated from single cells, the numbers of colonies in the culture should be as same as the numbers of SHs in the initially inoculated cells in culture. This means that the 2×10^6 initial cells used for the culture (/10 mm dish) contained about 5×10^3 SHs and generated about 7.2×10^4 proliferating SHs at day 12. The L.I. of SHs decreased after day 8 in culture and the numbers of proliferating cells in the SH colony were almost same at day 8 (approximately 57.3 cells/6.25 mm^2) and at day 12 (approximately 58.1 cells/6.25 mm^2). Although the number of proliferating SHs could be limited after day 8 in culture, the number of proliferating SHs at day 12 reached 15 times more than that immediately after isolation. We do not know the exact reason why proliferating SHs in culture did not increase after day 8 in this experiment. A possible reason is that present culture conditions may be unsuitable for every SH to keep proliferating. The cultured SHs could proliferate for a long-term, but they always generated mature hepatocytes under the current protocol.6 Suitable conditions for culturing SHs, in which all SHs can maintain proliferative activity without differentiation, should be investigated in a future experiment. Another possible reason is the existence of a specific cell population, even in the SHs, which can keep proliferating. Such specific SHs may be the only cells that can proliferate and maintain the activity. Similar cells, such as SH-like progenitor cells, appear in vivo when rats are exposed to a chemical agent such as retrorsine.[22] It would be interesting to determine if there is any difference between SHs from culture and in vivo SH-like progenitor cells. Both types of cells could engraft and repopulate in the recipient liver. Unlike oval cells and other hepatic stem cells,[23-25] no specific marker for SHs is known. Therefore, it is very difficult to distinguish them only with a marker. A relation between cell size and proliferative activity of the hepatocytes, which is the only landmark for SHs, in a liver repopulating model has also been debated.[26,27] Small-sized hepatocytes from the adult liver do not always proliferate and repopulate in the recipient.[26] This observation and ours again suggest the existence of a specific cell population in SHs, which can proliferate for a prolonged time.

Liver Repopulation

The aim of HT is to support liver functions and it could be an alternative to LT.[3-5] The liver is the best place for hepatocytes to express their functions. However, a space for cell engraftment is necessary in the recipient. Otherwise, donor cells have no chance to proliferate or repopulate to support liver functions. Therefore, several strategies have been used for making a space in the recipient.

Pretreatment with retrorsine, a pyrrolizidine alkaloid, combined with partial hepatectomy[10,22,28] was shown to be effective to replace nearly the whole liver with transplanted hepatocytes. However, the carcinogenicity of retrorsine proscribes its clinical application in humans. Mild hepatic damage is preferable in clinical treatment. After radiation-induced liver damage, massive liver repopulation is accomplished by hepatocyte transplantation combined with partial hepatectomy.[13] A surgical procedure such as hepatectomy is considered to be necessary to promote proliferation of donor cells and repopulation in the recipient. However, surgical invasiveness should be avoided for clinical treatment as much as possible. Al-

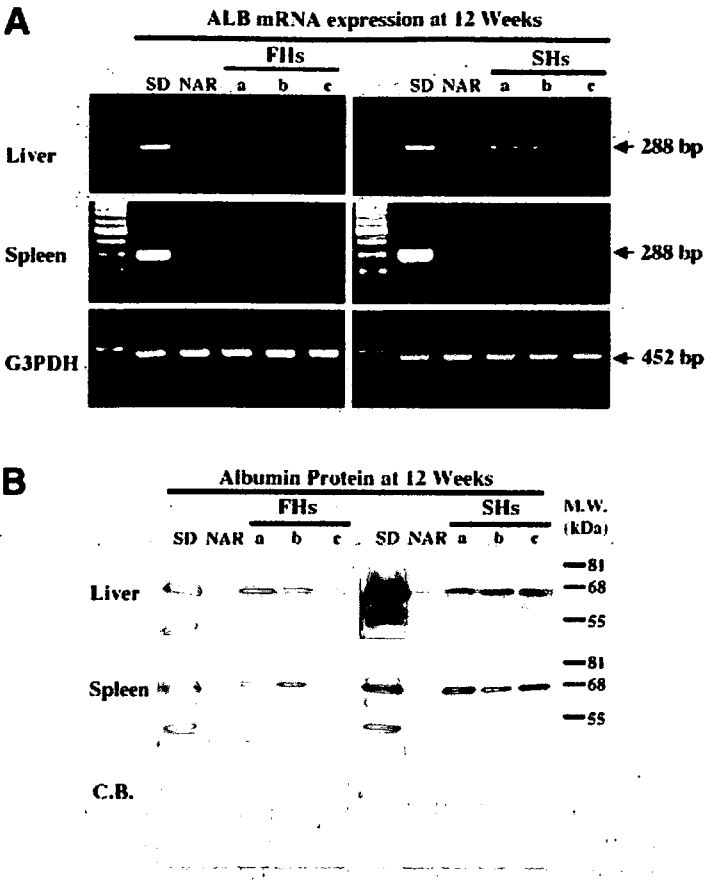

Figure 6. (A) RT-PCR analysis for albumin and G3PDH mRNA expression in NAR at 12 weeks after hepatocyte transplantation in the fresh hepatocyte (FH) group and small hepatocyte (SH) group. The photographs show three representative data from six different animals at 12 weeks. The control amplification of albumin mRNA was done using livers of male SD rats. Albumin mRNA was not detected in the spleen of the SD rat (data not shown). (B) Western blot analysis for albumin protein in NAR at 12 weeks after hepatocyte transplantation in the FH and SH groups. The photographs show three representative data from six different animals at 12 weeks. To each lane 10 mg of protein from the organ extracts was applied. The gels after protein transfer were stained with coomasie blue (C.B.).

though the efficacy of the hepatic repopulation was low in our protocol compared to previous reports,[13] it was high enough to support metabolic functions such as albumin production, as shown in this paper.

We observed that two rats showed near total hepatic repopulation at 12 weeks after HT in the FH group. This indicated that the adult liver could contain cells to repopulate the liver, which was consistent with other reports.[23,29,30] We do not know the exact reason why all rats did not show total hepatic repopulation. One possible reason could be that the damage due to hepatic irradiation was different in each animal. Because the rat liver is divided in nature, overlapping of the liver lobes is unavoidable. This suggests that the environment surrounding hepatic stem cells plays an important role in activating them to proliferate and repopulate. The activation of oval cells or SHs, which could be hepatic stem cells, and proliferation in vivo also depend on the environment where the proliferation of normal hepatocytes is inhibited.[22,24]

We do not know the reason why HT using SHs did not show total hepatic repopulation either. However, the trend of hepatic engraftment was similar in the FH and SH groups. This indicated that SHs could repopulate the liver. Our experiments might have been too short to observe total hepatic repopulation in the SH group. The ideal conditions for total hepatic repopulation should be investigated in future experiments.

We observed less engraftment in the NAR rat experiment than in the DPPIV rat experiment. The difference between the experiments was the use of immunosuppressive therapy. Controversial effects of cyclosporine on hepatocyte proliferation have been reported in vivo and in vitro.[31-33] We do not know the exact reason why we observed different results between the experiments; however, our findings suggested that immunosuppressive treatment might interfere with hepatocyte proliferation and repopulation.

Cell Source for HT

Primary FHs can be an ideal cell source for HT and liver repopulation. However, a large enough number of donor cells needs to be obtained for clinical treatment. Cells immortalized by gene transduction have been tested in experimental HT.[3] However, genetically manipulated cells are far from being available for clinical treatment because of safety issues. In addition, other stem cell sources[3] are unlikely to be candidates because of the time needed to express hepatic functions. SHs would be an ideal cell source as long as they could express liver functions as seen in vitro. We observed colony formation in the liver when SHs were transplanted into the NAR rat experiment. Cell engraftment in the SH group was less than in the FH group; however, the albumin production was similar. This suggested that cell-cell interaction between albumin-producing cells might play an important role in expression of albumin. Although SHs did not repopulate vigorously in vivo, the SH group achieved the same albumin pro-

TABLE 3. Albumin mRNA Expression and Protein in the Recipient Organs at 12 Weeks After HT

	FHs		SHs	
	mRNA	Protein	mRNA	Protein
Liver	32.37 ± 3.35%	16.75 ± 7.15%	35.57 ± 2.50%	19.97 ± 4.76%
Spleen	3.08 ± 1.14%	11.11 ± 3.22%	4.45 ± 2.98%	12.07 ± 3.49%

All data represent means ± standard deviations.
Organ samples were collected from 6 different animals and intensities of the PCR products and ECL signals were measured by densitometric analysis as described in Materials and Methods.

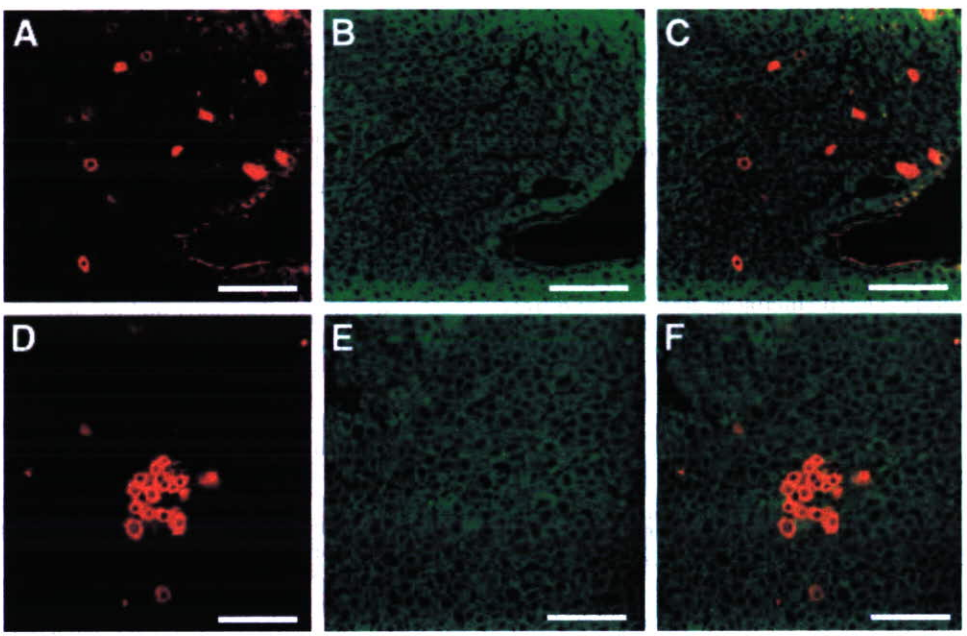

Figure 7. Confocal laser scanning microscopic analysis for ALB (red signals, A and D) and CK8 (green signals, B,E). The specimen was obtained from a female NAR liver at 12 weeks after transplantation using fresh hepatocytes (A-C) and small hepatocytes (D-F). All albumin-positive cells were consistent with CK8-positive cells (C,F). The scale bar represents 25 μm.

duction with fewer cells, which supports the idea that SHs could be an alternative cell source for HT.

The major advantage of SHs for HT could be the small number of cells, which could reduce the volume of the cells that need to be transplanted. A small volume of donor cells is preferable for any cell therapy because of the space needed for engraftment. In addition, another advantage of SHs could be their availability, as they are easily cryopreserved[9] and stored in comparison to FHs. However, the function of cryopreserved SHs in vivo needs to be investigated in a future study.

Fate of Transplanted Hepatocytes in the Spleen

Hepatocytes in the spleen were reported to disappear within a short period after HT.[34] Although the number of hepatocytes in the spleen decreased with time in our experiment, we detected albumin mRNA and protein in the spleen within a short period after HT at the different time points. This suggested that hepatocytes in the spleen after HT might support partial liver function until the time engrafted hepatocytes start to support it. HT using SHs may have advantages and disadvantages compared to HT using FHs. The mechanism of hepatic repopulation after HT through the spleen was explained by cell migration through the splenic vein to the recipient's liver.[35] When SHs were transplanted into the spleen, they could hardly escape from it because they tightly interacted and aggregated with each other. Therefore, hepatic engraftment using SHs is hard to achieve compared to using FHs, as seen in this paper. SHs in the spleen could support albumin production at a certain period, although the number of cells decreased gradually. They could not escape from the spleen to repopulate the liver; however, they stayed and engrafted in the spleen to express liver functions for a certain period. In any case, SHs could support liver functions in both the liver and spleen and could be an alternative to FHs as a cell source for HT.

In conclusion, HT using SHs showed hepatic repopulation similar to that using FHs. This suggested that both SHs and FHs contain hepatic cells that can repopulate the liver as if they were hepatic stem cells. In addition, HT using SHs supported liver functions such as albumin

correction at the same level as that using FHs. These observations support the hypothesis that SHs could be an alternative to FHs as a novel cell source for future HT.

ACKNOWLEDGMENTS

We thank Dr. Thomas Hui (McGill University, Montreal, Canada) and Dr. Yujo Kawashita (Nagasaki University, Nagasaki, Japan) for their valuable discussions, and Ms. Minako Kuwano for her technical assistance. We also thank to Dr. Hirohiko Ise (Shinshu University, Nagano, Japan) for his help in design of the Y-chromosome primers, and Mr. Kim Barrymore for his help in preparing this manuscript.

REFERENCES

1. Neuberger J. Developments in liver transplantation. Gut 2004;53:759-768.
2. Carithers RL, Jr. Liver transplantation: American Association for the Study of Liver Diseases. Liver Transpl 2000; 6:122-135.
3. Fox IJ, Roy-Chowdhury J. Hepatocyte transplantation. J Hepatol 2004;40:878-886.
4. Strom S, Fisher R. Hepatocyte transplantation: new possibilities for therapy. Gastroenterology 2003;124:568-571.
5. Horslen SP, Fox IJ. Hepatocyte transplantation. Transplantation 2004;77:1481-1486.
6. Mitaka T, Sato F, Mizuguchi T, Yokono T, Mochizuki Y. Reconstruction of hepatic organoid by rat small hepatocytes and hepatic nonparenchymal cells. Hepatology 1999;29:111-125.
7. Mizuguchi T, Mitaka T, Hirata K, Oda H, Mochizuki Y. Alteration of expression of liver-enriched transcription factors in the transition between growth and differentiation of primary cultured rat hepatocytes. J Cell Physiol 1998;174: 273-284.
8. Hino H, Tateno C, Sato H, Yamasaki C, Katayama S, Kohashi T, et al. A long-term culture of human hepatocytes which show a high growth potential and express their differentiated phenotypes. Biochem Biophys Res Commun 1999;256:184-191.
9. Ikeda S, Mitaka T, Harada K, Sugimoto S, Hirata K, Mochizuki Y. Proliferation of rat small hepatocytes after long-term cryopreservation. J Hepatol 2002;37:7-14.
10. Laconi E, Oren R, Mukhopadhyay DK, Hurston E, Laconi S, Pani P, et al. Long-term, near-total liver replacement by transplantation of isolated hepatocytes in rats treated with retrorsine. Am J Pathol 1998;153:319-329.
11. Gupta S, Rajvanshi P, Aragona E, Lee CD, Yerneni PR, Burk RD. Transplanted hepatocytes proliferate differently after CCl4 treatment and hepatocyte growth factor infusion. Am J Physiol 1999;276:G629-G638.
12. Wang X, Foster M, Al-Dhalimy M, Lagasse E, Finegold M, Grompe M. The origin and liver repopulating capacity of murine oval cells. Proc Natl Acad Sci U S A 2003;100:11881-11888.
13. Guha C, Sharma A, Gupta S, Alfieri A, Gorla GR, Gagandeep S, et al. Amelioration of radiation-induced liver damage in partially hepatectomized rats by hepatocyte transplantation. Cancer Res 1999;59:5871-5874.
14. Malhi H, Gorla GR, Irani AN, Annamaneni P, Gupta S. Cell transplantation after oxidative hepatic preconditioning with radiation and ischemia-reperfusion leads to extensive liver repopulation. Proc Natl Acad Sci U S A 2002;99: 13114-13119.
15. Takahashi M, Deb NJ, Kawashita Y, Lee SW, Furgueil J, Okuyama T, et al. A novel strategy for in vivo expansion of transplanted hepatocytes using preparative hepatic irradiation and FasL-induced hepatocellular apoptosis. Gene Ther 2003;10:304-313.
16. Ise H, Nikaido T, Negishi N, Sugihara N, Suzuki F, Akaike T, et al. Effective hepatocyte transplantation using rat hepatocytes with low asialoglycoprotein receptor expression. Am J Pathol 2004;165:501-510.
17. Seglen PO. Preparation of isolated rat liver cells. Methods Cell Biol 1976;13:29-83.
18. Lojda Z. Studies on dipeptidyl(amino)peptidase IV (glycylproline naphthylamidase). II. Blood vessels. Histochemistry 1979;59:153-166.
19. Miura K, Nagai H, Ueno Y, Goto T, Mikami K, Nakane K, et al. Epimorphin is involved in differentiation of rat hepatic stem-like cells through cell-cell contact. Biochem Biophys Res Commun 2003;311:415-423.
20. Masters DB, Griggs CT, Berde CB. High sensitivity quantification of RNA from gels and autoradiograms with affordable optical scanning. Biotechniques 1992; 12:902-906, 908-911.
21. Michalopoulos GK, DeFrances MC. Liver regeneration. Science 1997;276:60-66.
22. Gordon GJ, Butz GM, Grisham JW, Coleman WB. Isolation, short-term culture, and transplantation of small hepatocyte-like progenitor cells from retrorsine-exposed rats. Transplantation 2002;73:1236-1243.
23. Sell S. Heterogeneity and plasticity of hepatocyte lineage cells. Hepatology 2001;33:738-750.
24. Fausto N. Liver regeneration and repair: hepatocytes, progenitor cells, and stem cells. Hepatology 2004;39:1477-1487.
25. Laurson J, Selden C, Hodgson HJ. Hepatocyte progenitors in man and in rodents—multiple pathways, multiple candidates Int J Exp Pathol 2005;86:1-18.
26. Overturf K, Al-Dhalimy M, Finegold M, Grompe M. The repopulation potential of hepatocyte populations differing in size and prior mitotic expansion. Am J Pathol 1999; 155:2135-2143.
27. Katayama S, Tateno C, Asahara T, Yoshizato K. Size-dependent in vivo growth potential of adult rat hepatocytes. Am J Pathol 2001;158:97-105.
28. Oren R, Dabeva MD, Petkov PM, Hurston E, Laconi E, Shafritz DA. Restoration of serum albumin levels in Nagase analbuminemic rats by hepatocyte transplantation. Hepatology 1999;29:75-81.
29. Overturf K, al-Dhalimy M, Ou CN, Finegold M, Grompe M. Serial transplantation reveals the stem-cell-like regenerative potential of adult mouse hepatocytes. Am J Pathol 1997;151:1273-1280.
30. Wang J, Clark JB, Rhee GS, Fair JH, Reid LM, Gerber DA. Proliferation and hepatic differentiation of adult-derived progenitor cells. Cells Tissues Organs 2003;173:193-203.
31. Masuhara M, Ogasawara H, Katyal SL, Nakamura T, Shinozuka H. Cyclosporine stimulates hepatocyte proliferation and accelerates development of hepatocellular carcinomas in rats. Carcinogenesis 1993;14:1579-1584.
32. Lilja H, Blanc P, Demetriou AA, Rozga J. Response of cultured fetal and adult rat hepatocytes to growth factors and cyclosporine. Cell Transplant 1998;7:257-266.
33. Andres D, Diez-Fernandez C, Zaragoza A, Alvarez A, Cascales M. Induction of cell proliferation by cyclosporine A in primary cultures of rat hepatocytes. Biochem Pharmacol 2001;61:427-435.
34. Kusano M, Mito M. Observations on the fine structure of long-survived isolated hepatocytes inoculated into rat spleen. Gastroenterology 1982;82:616-628.
35. Lapidot T. Mechanism of human stem cell migration and repopulation of NOD/SCID and B2mnull NOD/SCID mice: the role of SDF-1/CXCR4 interactions. Ann N Y Acad Sci 2001;938:83-95.

Thermoreversible Gelation Polymer Induces the Emergence of Hepatic Stem Cells in the Partially Injured Rat Liver

Masaki Nagaya,[1, 4] Sunao Kubota,[2] Noboru Suzuki,[3] Katsuya Akashi,[1] and Toshihiro Mitaka[4]

Focal injury of the adult liver causes formation of granulomatous tissue and fibrosis. When thermoreversible gelation polymer (TGP) was applied to such defects of the rat liver, complete recovery of hepatic tissues was observed without granulation. We analyzed the mechanism of the regeneration. TGP is a chemically synthesized biocompatible polymer material whose sol-gel transition is reversible by changing the temperature. Cooled TGP was poured into a penetration lesion of the rat liver. Immunohistochemistry and polymerase chain reaction were carried out using tissues and cultured cells isolated from ductular structures. Immunocytochemical and ultrastructural analyses were also conducted. Seven days after TGP treatment, ductular reactions were observed around the wound and ductules elongated to the injured area. Cells in the structures were alpha-fetoprotein (AFP) positive, albumin$^+$, CK19$^+$, c-Kit$^+$, and Thy1$^+$. Hepatocyte-like cells possessing glycogen appeared around the tips of the ductules from day 9. The defect was completely replaced with hepatocytes by day 28. Cells isolated from the ductules expressed Musashi-1, c-Kit, Thy1, AFP, albumin, transferrin, connexin 43, and CK19. When the cultured cells were covered by TGP, they rapidly proliferated to form colonies, whereas without TGP cells gradually died. Morphologically and ultrastructurally the cells were similar to hepatocytes. They expressed not only albumin and transferrin but TAT, CYP2E1, and CCAAT/enhancer binding protein α. Some cells formed bile canaliculus-like structures. In conclusion, TGP may trigger the initiation of hepatic stem cells in biliary ductules, and stem cell activation may occur even in the regeneration of the normal liver. (HEPATOLOGY 2006;43:1053-1062.)

The mechanisms of regeneration in focal liver injury are not well understood. We found that the defect made by focal injury was usually replaced by granulomatous tissue. When we used thermoreversible gelation polymer (TGP) as a sealing material for the injury, efficient regeneration occurred without any granulation.[1] TGP is a chemically synthesized biocompatible polymer material.[2] It is soluble below a lower critical solution temperature (LCST) and becomes solid above the LCST. When soluble TGP is applied, it can infiltrate into any part. Thereafter, it immediately changes into gel at body temperature and causes complete sealing of the defect, leading to efficient regeneration of the liver.[1] However, the mechanisms of the regeneration with TGP treatment have largely remained unknown.

The liver appears to have three distinct mechanisms of regeneration in response to loss of hepatocytes: (1) Mature hepatocyte (MH)s proliferate in case of partial hepatectomy and centrolobular injury by hepatotoxins.[3-5] Surviving hepatocytes immediately proliferate and restore the original mass[4]; (2) When the proliferation of hepatocytes is inhibited by some toxins such as 2-acetylaminofluorene, hepatic growth stimulation results in emergent ductules, and the cells in the ductules gradually migrate into the hepatic parenchyma.[3-5] "Oval cells" or "ductular hepatocytes" are involved in the ductular reaction in rodents.[5,6] These cells may be derived from putative stem cells and may differentiate into hepatocytes; (3) Bone

Abbreviations: TGP, thermoreversible gelation polymer; LCST, lower critical solution temperature; MH, mature hepatocyte; NIH, National Institutes of Health; HE, hematoxylin-eosin; PAS, periodic acid-Schiff; TEM, transmission electron microscopy; AFP, alpha-fetoprotein; CK19, cytokeratin 19; PCNA, proliferating cell nuclear antigen; C/EBPα, CCAAT/enhancer binding protein α; MRP2, multidrug-resistance associated protein 2; BEC, bile epithelial cell; BDL, common-bile-duct ligation; NT, no treatment; CG, collagen gel; FG, fibrin glue; POD, post operative day; BC, bile canaliculi.

From the [1]Department of Emergency and Critical Care Medicine; the [2]Department of General Surgery; the [3]Department of Immunology and Medicine; St. Marianna University, School of Medicine, Kawasaki, and the [4]Department of Pathophysiology, Cancer Research Institute, Sapporo Medical University School of Medicine, Sapporo, Japan.

Received October 14, 2005; accepted February 13, 2006.

Supported by Grants-in-Aid from the Ministry of Education, Culture, Sports, Science and Technology of Japan (15790708 to M.N. and 14370393, 17390353 to T.M.) and the Marumo Fund (to M.N).

Address reprint requests to: Masaki Nagaya, M.D., Ph.D., Department of Emergency and Critical Care Medicine, St. Marianna University, School of Medicine, Kawasaki 261-8511, Japan: E-mail: m2nagaya@marianna-u.ac.jp; fax: (81) 44-979-1522.

Published online in Wiley InterScience (www.interscience.wiley.com).

DOI 10.1002/hep.21153

Potential conflict of interest: Nothing to report.

marrow–derived cells may participate in hepatic regeneration.[4,5,7]

Here we report that, in the hepatic regeneration of focal injury by TGP, ductular reactions are initially induced, and hepatic stem cells involved in the ductules may differentiate into hepatocytes. In addition, cells isolated from the ductules induced by TGP treatment can rapidly proliferate and differentiate into hepatic cells when the cells are covered by TGP. Thus, hepatic stem cells may participate in hepatic regeneration even when no hepatotoxins are involved in the injury.

Materials and Methods

Animals and Surgery. Adult male Fisher 344 rats were obtained from Charles River (Atsugi, Kanagawa, Japan). All animals received humane care, and the experimental protocol was approved by the Committees of Laboratory Animals of St. Marianna and Sapporo Medical Universities and was in accordance with National Institutes of Health (NIH) guidelines. The total number of sacrificed rats was over 150, and at least five animals/point were examined. A penetrating, 4-mm-diameter defect was made in left middle lobe of the liver at a distance of 10 mm from lobular edges. The rats were then randomly assigned into three groups: penetration alone (control), penetration filled with fibrin glue (FG, Kaketsuken, Kumamoto, Japan), and penetration filled with TGP (TGP, Mebiol, Tokyo, Japan). FG and TGP (0.5 mL) were poured into the penetrated site.

Preparation of TGP. N-isopropylacrilamide, Eastman Kodak, New York, NY) was recrystallized from acetone and copolymerized with N-acryloxysuccinimide (Kokusan Chemical, Tokyo, Japan) to provide an activated form of Poly- N-isopropylacrilamide. Polymerization was carried out in $CHCl_3$, using azobisisobutyronitrile as the initiator. The activated copolymer was precipitated with diethylether and recovered. Then the copolymer and diamino-polyethylene glycol (Kawaken Fine Chemicals, Tokyo, Japan) were dissolved in $CHCl_3$ and reacted. The byproduct, N-hydroxylsuccinimide, was removed and the remaining solution was lyophilized to yield TGP. Saline was added to the TGP to adjust it to 5.5 % (wt/wt). The LCST was approximately 20°C[2], and toxicity of TGP was not observed.[1]

Histology. Liver tissues were obtained from the injured lobe, and other lobes were used as a control. Liver specimen (diameter 10 mm) surrounding the injured region was enucleated in a cylindrical shape. The specimen was cut in half, and both paraffin and frozen samples were prepared. The ventral halves of the specimens were fixed with 4% paraformaldehyde in phosphate-buffered saline and embedded in paraffin. To evaluate the size of the injury lesion, the area of fibrosis in hematoxylin-eosin (HE)-stained sections was measured and analyzed using a light microscope equipped with a CCD camera and AxioVision AC Rel. 4.1 software (Carl Zeiss, Jena, Germany). In addition, to evaluate the hepatic lobule size, the distance between portal veins was measured. The proximal portion less than 3 mm from the injured site and the distal portion farther than 5 mm from the injured site were evaluated. Periodic acid-Schiff (PAS)-staining was performed to examine the production of glycogen. Diastase was applied to test whether PAS-positive materials were glycogen.[8] The procedure used for transmission electron microscopy (TEM) was previously described.[9]

Immunostaining. Antibodies to c-Kit (Santa Cruz, CA), Thy1 (Pharmingen, Hamburg, Germany), α-fetoprotein (AFP; Dako Cytomation, Kyoto, Japan), albumin (Dako Cytomation), cytokeratin 19 (CK19; Novocastra Laboratories, Newcastle, UK and a gift of Dr. A. Miyajima, Tokyo University, Japan), proliferating cell nuclear antigen (PCNA; Dako Cytomation), Ki67 (Pharmingen), CCAAT/enhancer binding protein α (C/EBP α; Santa Cruz), and multidrug-resistance associated protein 2 (MRP2; Alexis Biochemichals, San Diego, CA) were used. The methods used for immunohistochemistry and immunocytochemistry were previously described.[9] 3, 3′-Diaminobenzidine and BCIP/NBT (Dako Cytomation) were used as a substrate for colorization. $Alexa^{488}$-conjugated and $Alexa^{594}$-conjugated antibodies (Molecular Probes, Eugene, OR) were used as secondary antibodies.

CK19 and Albumin Double-Positive Cells in the Ductules. Immunohistochemistry for CK19/albumin was carried out. The number of $CK19^+$/$albumin^+$ cells in the ductules in the upper right quadrant area was counted, which included part of the injured areas. Simultaneously, we measured the size of the area by using NIH image software.

Isolation and Culture of Ductular Cells. Intrahepatic biliary epithelial cell (BEC)s were separated from normal, common-bile-duct-ligated (BDL), and TGP-treated rat livers. To isolate the cells from the injury lesion, two-step liver perfusion[9] was initially carried out 1 week after operation. The tissue was enucleated in a cylindrical shape (diameter 10 mm) surrounding the injured site and transferred into a Petri dish. After hepatocytes were removed, the remnant tissues were collected, transferred into a flask, and then treated with collagenase, dispase (Godo Shyusei, Tokyo, Japan) and hyaluronidase (Sigma, St Louis, MO) for 30 minutes. The digested tissues were suspended in Dulbecco's modified Eagle's medium and centrifuged at 150*g* for 10 minutes. The pellet was resuspended in the medium, filtered

Table 1. Sequences of PCR Primers

Primer	Sequence (5'-3')	Anneling Temperature (°C)	PCR Product (bp)
GAPDH	CCATCACCATCTTCCAGGAG	60	576
	CCTGCTCACCACCTTCTTG		
Musashi-1	ATGCCATGCTGATGTTCGAC	60	255
	ACCCTGGGTAACCTAACATG		
c-Kit	CATCATGGAAGATGACGAG	60	281
	CAAATGTGTACACGCAGCTG		
Thy1	ACAAGCTCCAATAAAACTATCAATGTGAT	60	84
	GGAAGTGTTTTGAACCAGCAGG		
AFP	TGAAATTTGCCACGAGACGG	60	272
	TGTCATACTGAGCGGCTAAG		
Albumin	GACAAGTTATGCGCCATTCC	60	288
	ACTGGGTCAGAACCTCATTG		
Transferrin	TGTCTGAGCATGAGAACACC	60	299
	GTTCAGCTGGAAGTCTGTTC		
TAT	TACTCAGTTCTGCTGGAGCC	60	471
	GCAAAGTCTCTAGAGAGGCC		
CYP2E1	AGCACAACTCTGAGATATGG	60	365
	ATAGTCACTGTACTTGAACT		
CYP3A1	CAGCTCTCACACTGGAAACCTGGG	60	689
	CTCATATATTTGGGGTGAGGAATGG		
CX43	GGAAAGTACCAAACAGCAGC	60	348
	AGGACTTGTCATAGCAGACG		
CK19	ATGACTTCCTATAGCTATCG	60	340
	CACCTCCAGCTCGCCATTAG		
CX18	GGACCTCAGCAAGATCATGGC	60	515
	CCACGATCTTACGGGTAGTTG		
HNF3α	TTCGGAGTTGAAGTCTCCAG	60	218
	CATATGCCTTGAAGTCCAGC		
HNF4	TCTACAGAGCATTACCTGGC	60	614
	TGAGGGGAAGATGAAGACGG		
C/EBPα	TTCCAGATCGCACACTGCCC	60	404
	TGACCAAGGAGCTCTCAGGC		
HNF6	GACAAATGGCAGGACGAGGG	60	681
	AGCGTACTGGTTTAGGTGCC		

NOTE. GAPDH was used as an internal control.

through 70-μm nylon mesh, and small cell aggregates on the mesh were selectively picked up using a pipette. The cell aggregates were suspended in Dulbecco's modified Eagle's medium supplemented with 10% fetal bovine serum, 10 mmol/L nicotinamide, 1 mmol/L ascorbic acid 2-phosphate, 10 ng/mL epidermal growth factor (Collaborative Research, Lexington, MA), 10^{-7} mol/L dexamethasone, 0.5 μg/mL insulin, and antibiotics. Then 200 cell aggregates were plated on a 35-mm dish. Seven days after plating, the dishes were randomly divided into 3 groups: no treatment (NT), cells overlaid with collagen gel (CG), and cells overlaid with TGP gel (TGP). The specific gravity of both collagen gel and TGP was adjusted to 1.06 mg/mL.

Polymerase Chain Reaction. Total RNA was isolated from ductules and cultured cells, and reverse transcriptase-polymerase chain reaction was conducted as previously described.[10] Primers are listed in Table 1.

Colony Counts. We measured colony number and size using a phase-contrast microscope (Olympus Optical, Tokyo, Japan) equipped with a CCD camera.

Statistics Analysis. Data are shown as mean ± SEM. ANOVA and Fisher's protected least significant difference test were used, and a P value $<.05$ was considered significant.

Results

Histology of the Liver Injury. At day 28, we macroscopically observed complete recovery of liver tissue in the TGP group, whereas in livers of both the control and FG groups fibrosis was apparent in the lesions. As shown in Fig. 1, in the control group, the hole was left open, and exudates accumulated at postoperative day 3 (POD 3, Fig. 1B). Thereafter, inflammatory and fibroblastic cells gradually gathered and formed granulomatous tissue at POD 7, which became larger and more prominent at POD 14 (Fig. 1C) and POD 28 (Fig. 1D). In the FG group, inflammatory cells and fibroblastic cells invaded the FG at POD 3 (Fig. 1F). The FG remained in the center of the lesion and fibrosis was observed at the periphery of the defect at POD 14 (Fig. 1G). Granuloma-

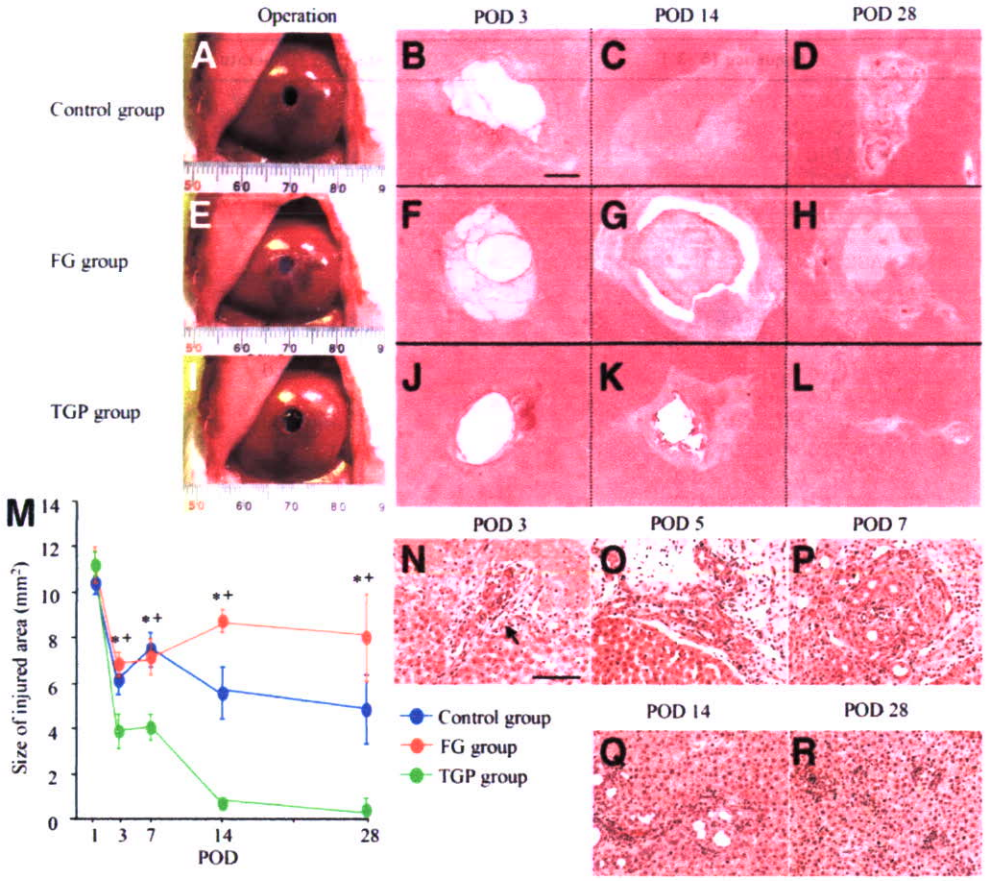

Fig. 1. Histological analysis of the partially injured rat liver filled with TGP. A penetrating wound was made in the left middle lobe (A). The hole was left open (control group). Exudates and coagulation accumulated in the injury site at POD 3 (B). Inflammatory cells and fibroblasts gradually formed granulomatous tissue, and scar formation then became evident at POD 14 (C) and POD 28 (D). Fibrin gel was poured into the lesion (E; FG group). The inflammation was evident inside and around the gel at POD 3 (F). FG changed to granuloma and the size of the injured area was enlarged at POD 14 (G). Hepatic regeneration did not occur at POD 28 (H). The hole was filled with TGP (I; TGP group). A thin layer of connective tissues surrounding TGP was observed at POD 3. The area of TGP became small and the injured area gradually shrank at POD 14 (K). Most of the injured area was replaced with hepatic cells, and only a small amount of fibrosis remained at POD 28 (L). B-D, F-H, and J-L show HE staining at the same magnification. Scale bar, 1 mm. Change of the size of the injured area after operation in each group (M). Bars show mean ± SEM of five samples. TGP versus *Control and +FG, $P < .05$. Histological appearance of the liver tissues treated with TGP: Ductular reactions (an arrow) emerged at POD 3 (N). They elongated from the portal areas located at the boundary between intact hepatocytes and dead cells. The ductules extend toward the injured area at POD 5 (O). The cells in ductular reactions became columnar-like structures at POD 7 (P). The hepatocyte-like cells increased around the ductules at POD 14 (Q). On POD 28, most ductules have disappeared and the lesion is almost completely replaced with hepatocytes (R). N-R are the same magnification. Scale bar, 100 μm. TGF, thermoreversible gelation polymer; POD, postoperative day; FG, fibrin glue; HE, hematoxylin-eosin.

tous tissue was observed even at POD 28 and no replacement of hepatocytes was observed (Fig. 1H). In the TGP group, the TGP-occupied area was observed as a vacant area (Fig. 1J) that gradually shrank with time (Figs. 1J-L). Between the vacant area and intact hepatocytes, a relatively narrow area of tissue consisting of epithelial and fibroblastic cells, some inflammatory cells, and fibrosis were observed at POD 14 (Fig. 1K). Although a small amount of fibrosis remained, the lesion was almost completely replaced by hepatocytes at POD 28 (Fig. 1L). As shown in Fig. 1M, the size of the injured area dramatically decreased in the TGP group, whereas it did not change in the FG group and decreased by half in the control group.

To examine whether remnant MHs surrounding the injured area participated the regeneration, we measured the sizes of neighboring lobules. Lobules not only proximal but also distal to the injury were not enlarged during regeneration (data not shown).

As shown in Fig. 1N, ductular reactions were first observed at POD 3 in the TGP group. The ductules might have originated from the presumptive area of portal triads and elongated toward the center of the injury. The length and the number of the ductules gradually increased until POD 7 (Fig. 1O-P). Compared with normal BECs, the cells in the ductules had relatively large cytoplasms and round nuclei, although both were smaller than those in

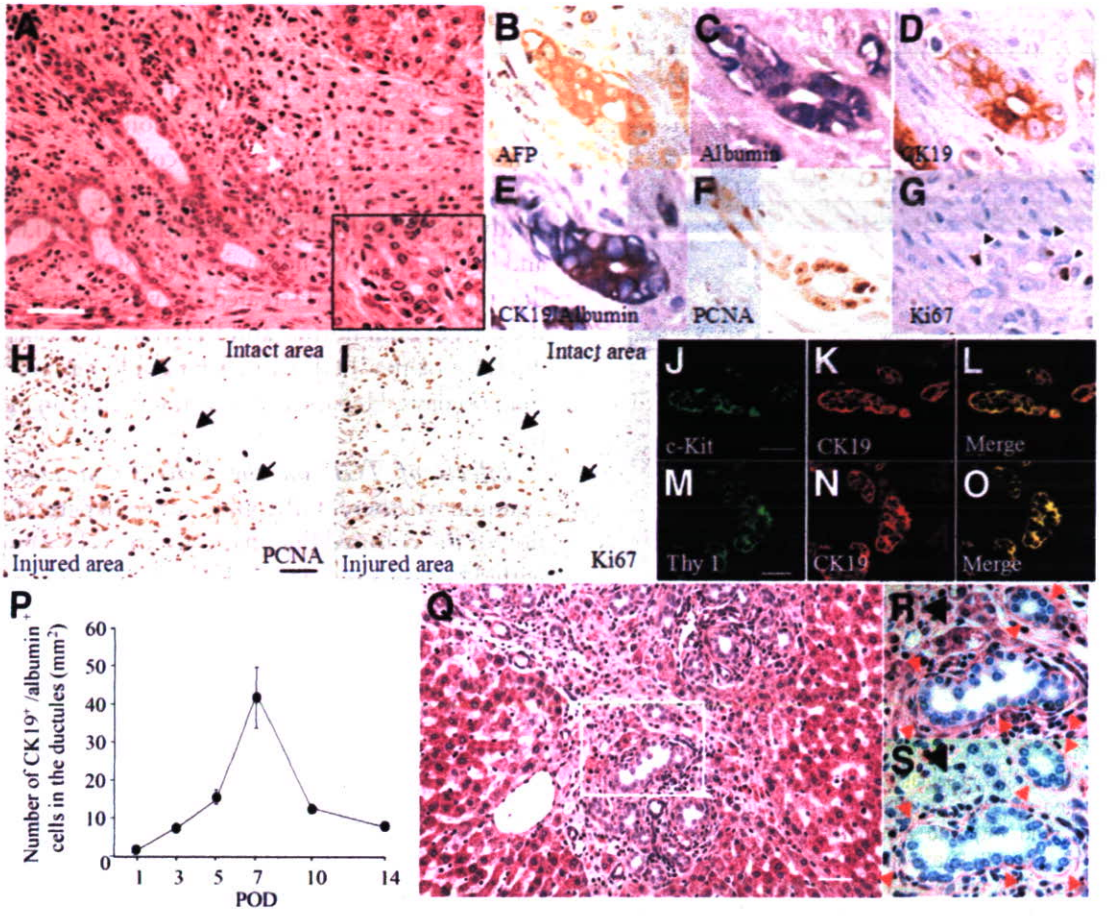

Fig. 2. Characterization of the cells in ductular reactions induced by TGP. Serial sections of the liver tissues were prepared and immunohistochemistry was carried out at POD7. HE staining (A): inset shows the enlargement of the location indicated by white arrowheads. Scale bar, 100 μm. Immunohistochemistry for AFP (B), albumin(C), CK19 (D), PCNA (F, H), and Ki67 (G, I). (E) Double staining of CK19 and albumin. Arrowheads in F and G show Ki67$^+$ nuclei. Immunohistochemistry for PCNA (H) and Ki67 (I) shows that relatively few adjacent hepatocytes (intact area) have positive nuclei at POD 7. Arrows in H and I show the boundary between the injured area and intact area. Scale bar, 100 μm. Fluorescent double immunohistochemistry for c-Kit/CK19 (J-L) and Thy1/CK19 (M-O) of the cells in ductular reactions at POD 7. Scale bar, 100 μm. (P) The number of CK19$^+$/albumin$^+$ cells in the ductules in the upper right quadrant area was counted, which included part of the injured areas. Simultaneously, we measured the size of the area (mm^2) by using NIH image software. Based on the above measurements, we calculated cells/mm^2. The peak of the number was observed at POD 7. We used five rats at each time point, and one slide per rat was prepared for the measurement. The results are shown as mean $\pm$ SEM of five rats. PAS-staining of the cells in ductular reactions at POD 9 (Q-S). (R and S) Enlargement of the square shown in Q. The section was pretreated with diastase before PAS-staining (S). Pinkish granules are observed in the cytoplasm of hepatocyte-like cells around ductules (R, black arrowhead), and basement membrane (positive lines) is surrounding the ductules (red arrows). The pinkish granules in hepatocyte-like cells disappeared after diastase treatment (S, black arrowhead), whereas the linear staining remained around the ductules (S, red arrows). Scale bar, 100 μm. TGF, thermoreversible gelation polymer; POD, postoperative day; FG, fibrin glue; HE, hematoxylin-eosin; AFP, alpha-fetoprotein; PCNA, proliferating cell nuclear antigen; SEM, scanning electron microscopy; PAS, peroidic acid-Schiff.

MHs. The cells in ductules changed their configuration from rectangular to columnar, and hepatocyte-like cells appeared surrounding the ductules (Fig. 1P-Q). At POD 28, the injury lesion was replaced by hepatocytes, and most ductules disappeared. No ductular proliferation was detected in either the control or FG group. Characterization of the cells in ductular reactions was carried out by immunostaining. At POD 7, most cells had CK19, albumin, and AFP (Fig. 2B-E). In addition, 68% and 72% of CK19$^+$ cells in the ductules were c-Kit$^+$ and Thy1$^+$, respectively (Fig. 2J-O). To examine the growth activity of the cells, immunostaining for PCNA and Ki67 was performed. As shown in Fig. 2F-I, many cells in ductular reactions possessed PCNA$^+$ or Ki67$^+$ nuclei, whereas relatively few MHs surrounding the ductular reactions had positive nuclei. The number of CK19$^+$/albumin$^+$ cells in the ductules was counted and the peak was observed at POD 7 (Fig. 2P). The largest numbers of c-Kit$^+$, Thy1$^+$, AFP$^+$, PCNA$^+$ and Ki67$^+$ cells were also observed at POD 7 (data not shown).

As shown in Fig. 2Q-R, hepatocyte-like cells surrounding the ductules appeared at approximately POD 9. To

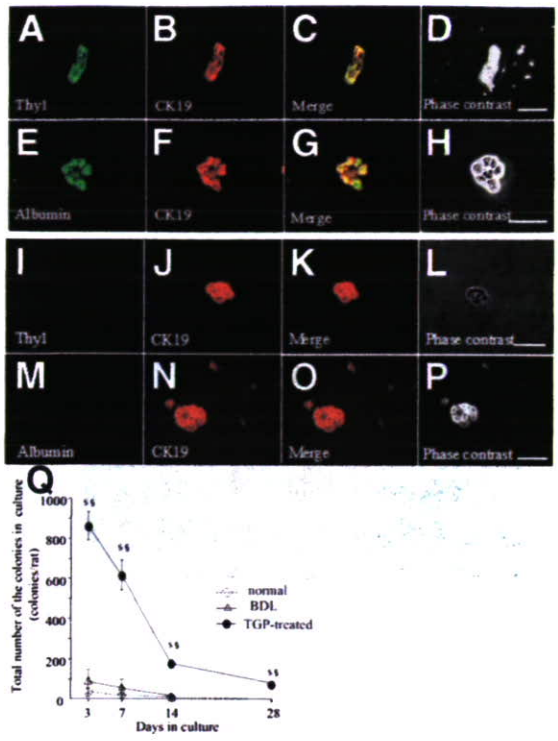

Fig. 3. Characterization of isolation and culture of the ductular cells from a TGP-treated rat liver. Double immunostaining of the cells for Thy1/CK19 (A-C and I-K) and albumin/CK19 (E-G and M-O) was conducted. (D, H, L, and P) Phase-contrast photos of the corresponding cells. Approximately 72% of the isolated cells were Thy1$^+$. CK19$^+$ cells from a normal rat liver were Thy1$^-$ (I) and albumin$^-$ (M). Scale bars, 100 μm. (Q) Total number of colonies per rat. The cells were isolated from normal rats (normal), rats with BDL, and rats treated with TGP (TGP-treated). The ordinate shows the total number of colonies per rat. The points show mean ± SEM of five independent experiments using five rats. TGP versus normal[$] and BDL[§], $P < .05$. TGF, thermoreversible gelation polymer; BDL, bile duct ligated.

examine whether the cells were hepatocytes, PAS staining was performed (Fig. 2R-S). Reddish granules in cytoplasm (Fig. 2R) were observed, and the materials were digested by diastase (Fig. 2S). Conversely, basement membrane surrounding the ductules was not digested. The results proved that the hepatocyte-like cells possessed glycogen in their cytoplasm and were hepatocytes.

Isolation and Culture of Cells in TGP-Induced Ductules. Cells in ductules were isolated from the TGP-treated rat livers and formed small aggregates. To characterize the cells, immunocytochemistry for CK19 and Thy1 was conducted. We found that 89% and 84% of the attached cells were CK19$^+$ and Thy1$^+$, respectively (Fig. 3A-D). Moreover, most CK19$^+$ cells expressed both albumin (Fig. 3E-H) and c-Kit (data not shown). When the same manipulation was performed for rats of the control and FG groups, although few cells were isolated, all cells died in early culture. Therefore, we used BECs from normal and BDL rats as controls. Although all CK19$^+$ BECs isolated from normal and BDL rats survived more than 2 weeks, they did not express Thy1 or albumin (Fig. 3I-P). After plating, the cells from the TGP-treated rats started to grow from day 3 and formed colonies. Colonies sometimes fused and formed a large colony. The number of colonies decreased with time in culture but was significantly higher in the TGP-treated than in both the normal and BDL rats. As shown in Fig. 3Q, the number of ductules from a TGP-treated rat was clearly larger than those from both normal and BDL rats. The cells from the ductules of the TGP-treated rat could survive for more than 60 days. Hepatic cells did not contaminate this culture.

Effects of TGP on the Cells From Ductules. To examine whether TGP could induce hepatic differentiation of the cultured ductular cells, the cells were overlaid with TGP gel from day 7. The cells extensively proliferated, and the colonies became large (Fig. 4D). To exclude the possibility that any gel overlay could induce the differentiation, collagen gel was used as a control. The number of the surviving colonies in all cultures from the 3 groups rapidly decreased with time in culture (Fig. 4E). However, after TGP overlay, the degree of the decrease was suppressed. The slight decrease in the number of colonies in TGP was due to the fusion of neighboring colonies and, therefore, each colony became a large one. Approximately 20 colonies/dish survived in TGP and continued proliferating with time in culture (Fig. 4F). More than 1 month later, cells with large cytoplasm appeared around the periphery of some colonies (Figs. 4G-H). The cells expressed not only albumin but also C/EBPα, which is expressed in differentiated hepatocytes (Fig. 4I). As shown in Fig. 4J, translucent belts were sometimes observed between large cells. These cells expressed albumin (Fig. 4L), and MRP2 was immunocytochemically stained along the structure (Fig. 4K). Therefore, the structures might have been bile canaliculi (BC). Most colonies in NT and CG disappeared by day 42.

To observe the cultured cell ultrastructures, perpendicular sections were prepared using the semithin sections of the samples for TEM. As shown in Fig. 5A, a one- or two-cell layer of columnar cells was arranged on connective tissues, and the cells were larger than 10 × 10 μm, and thus perhaps larger than BEC and smaller than MH. Transversal sections also showed that the colonies consisted of relatively large cells (Fig. 5B). Although the existence of peroxisomes was not proved, the cells possessed many organella such as mitochondria and rough endoplasmic reticulum. In addition, BC-like structures with many microvilli were observed between the cells (Fig. 5C).

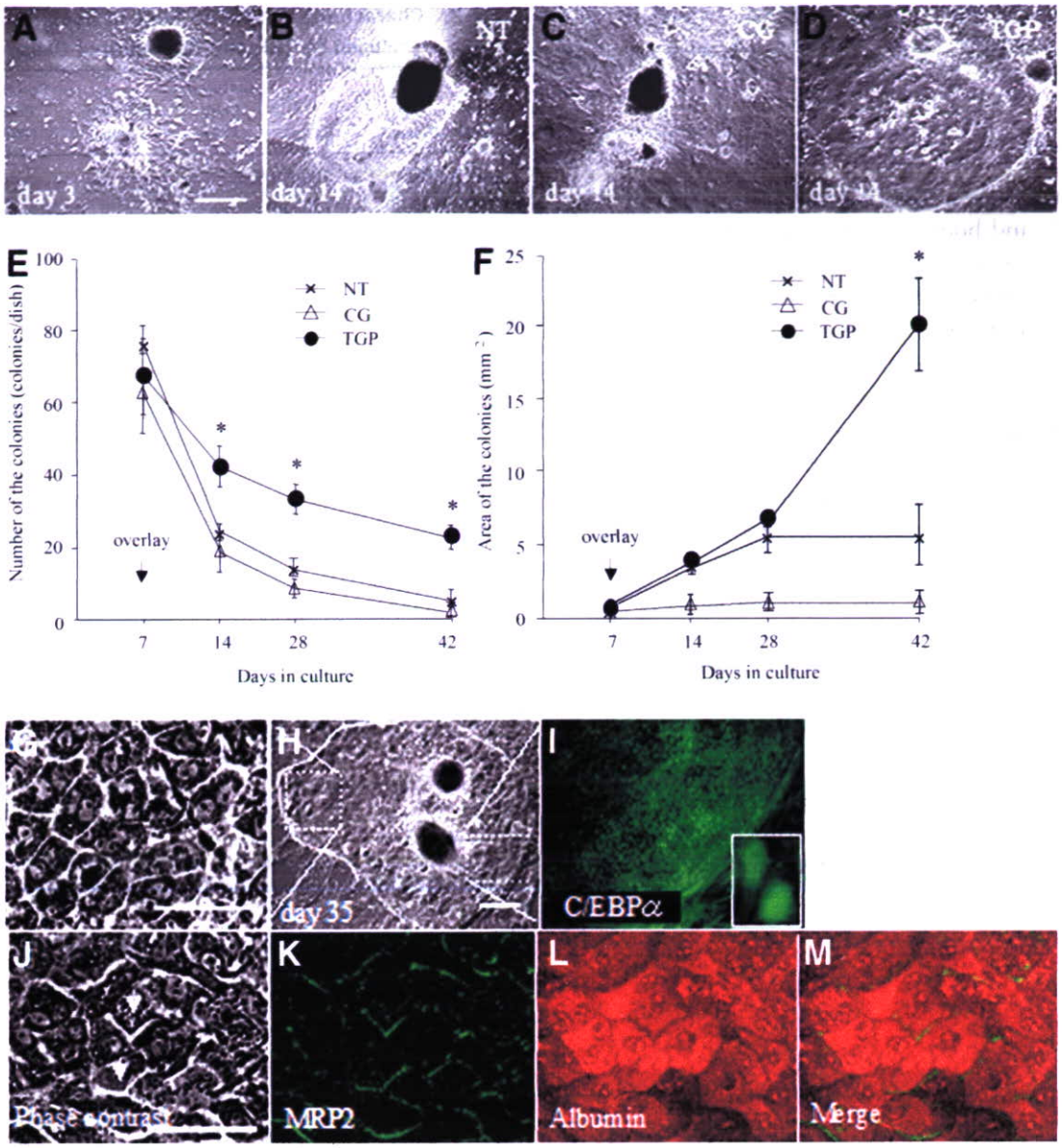

Fig. 4. Culture of the cells isolated from a rat liver treated with TGP. The isolated cells were plated on dishes. The cells initially formed small aggregates and expanded to form colonies with time in culture. Seven days after plating, the cultures were randomly assigned into three groups: Cells were overlaid with nothing (NT), 1 mL collagen gel (CG), and 1 mL TGP gel (TGP). The cells proliferated to form colonies (A), and the colonies continued expanding (B). The cells under CG marginally grew from aggregates (C). The cells under TGP showed rapid expansion to form large colonies (D). The number (E) and the size (F) of the colonies in the cultures were measured. Bars show mean ± SEM of five independent experiments. The number of the colonies at day 3 in each group (NT, CG, and TGP) was 170.8 ± 5.3, 161.6 ± 10.4, and 151.6 ± 7.3, respectively. The area of the colonies at day 3 in each group (NT, CG, and TGP) was 0.26 ± 0.06, 0.21 ± 0.03, and 0.23 ± 0.04 mm^2, respectively. TGP versus *both groups, $P < .05$. Characterization of the cells overlaid with TGP at day 35 (G-M). (G) Enlargement of the location in H indicated by the dotted rectangle. Cells with relatively large cytoplasm are mainly observed in peripheral portions of expanding colonies. Many cells have two nuclei. Scale bar in G, 100 μm. Scale bar in H, 1 mm. Fluorescent immunocytochemistry for C/EBPα (I), MRP2 (K), and albumin (L) was conducted in the cells overlaid with TGP. (I) Enlargement of the portion shown in H indicated by the dotted rectangle. Inset shows a high magnification of the positive nuclei. A phase-contrast photograph of the colony shows that relatively large cells have translucent belts (arrows) between the cells (J). Scale bar, 100 μm. (J and K-M) Phase-contrast micrograph and double immunostaining for MRP2 and albumin of the same cells, respectively. The cells with large cytoplasm are positive for albumin and form translucent belts between the cells. MRP2 is expressed along the belt-like structures. TGF, thermoreversible gelation polymer.

As shown in Table 2, reverse transcription polymerase chain reaction indicated that the isolated cells expressed albumin, transferrin, HNF3α, HNF4, CYP1A1 (hepatic markers), CX43, CK19, CK18 (cholangiocyte markers), AFP, c-Kit, Thy1, and Musashi-1 (immature cell markers).[11] The cells in NT lost the immature cell markers at day 35, and marker genes of differentiated hepatocytes such as TAT, C/EBPα, and CYP2E1 were not detected.

However, when the cultured cells were overlaid with TGP, TAT, C/EBPα, and CYP2E1 genes were expressed at day 35.

Discussion

In rodents and humans, a relationship exists between liver growth and body mass. In resections involving the removal of 40% to 70% of the rodent liver, a linear relationship is seen between the amount of removed tissue and the extent of hepatocyte proliferation. However, the removal of up to 30% of the liver fails to cause a synchronized wave of hepatocyte proliferation after the operation, although the liver eventually regains its mass.[12] In human liver surgery, enucleation of hepatic tumors is performed, and accidental liver injury sometimes occurs. However, the mechanism of the regeneration of a partial defect in the liver is not well understood. Recently, we realized that, when TGP was used as a filler in the partially penetrated liver, we could not find any trace of the injury within 1 month. In the process of hepatic regeneration with TGP, ductular reactions initially appeared at the margins of the area filled with TGP, and the number of inflammatory cells was not large. In addition, although many cells in the ductules showed positive staining of cell cycle–related proteins, proliferation of intact hepatocytes surrounding the injury lesion was relatively few, and the size of the lobules proximal to the lesion did not change after the treatment. This phenomenon was observed only when TGP was used as the filler in the partial defect. When the focal lesion remained untreated (control), exudates immediately filled the space accompanying many inflammatory cells and were then gradually replaced with granulomatous tissue. Even after 1 month, the lesion showed scar formation, and the scar remained for a long time. When FG was used as the filler, a large area of fibrosis in the lesion remained in all rats. Therefore, we considered that the cells in ductular reactions might play an important role in the regeneration of the TGP-treated liver.

The emergence of atypical ductular cells (so-called "ductular reactions") has been reported in some experimental conditions of rodents[13,14] and human liver diseases. For the cellular origin of the ductular reactions, oval cells,[3-5] ductular metaplasia (transdifferentiation from hepatocytes into ductular cells),[13,15] and ductular hepatocytes[3,6,16] have been suggested; however, this is still controversial. In the current experiment, the cells in ductular structures induced by TGP possessed many hepatic proteins such as albumin, transferrin, CYP1A1, HNF3α, and

Table 2. Characterization of the Cells in Ductular Reactions Induced by TGP and the Cultured Cells

Marker Genes	BECs	Cultured Cells (NT)	Isolated Cells	Cultured Cells (TGP)	MHs
Progenitor cells					
Musashi-1	−	−	+	−	−
Oval-cell related					
c-Kit	−	−	+	−	−
Thy1	−	−	+	−	−
AFP	−	−	+	−	−
Hepatocytes					
Albumin	−	+	+	+	+
Transferrin	−	+	+	+	+
TAT	−	−	−	+	+
CYP2E1	−	−	−	+	+
CYP3A1	−	−	−	−	+
Cholangiocytes					
CX43	+	+	+	+	−
CK19	+	+	+	+	−
CK18	+	+	+	+	+
Transcription factors					
HNF3α	−	+	+	+	+
HNF4	−	+	+	+	+
C/EBP α	−	−	−	+	+
HNF6	+	+	+	+	+

NOTE. Gene expression of cell lineage markers was analyzed by semi-quantitative RT-PCR. Total RNA was isolated from BECs (normal rat), the isolated cells in ductular reactions induced by TGP, the cultured cells without overlay (NT) and with TGP (TGP), and MHs (normal rat). Three separate experiments were performed, and the results were reproducible.

−, not detectable; +, detectable.

Abbreviations: BEC, bile epithelial cell; TGP, thermoreversible geiation polymer; NT, no treatment; MH, mature hepatocyte.

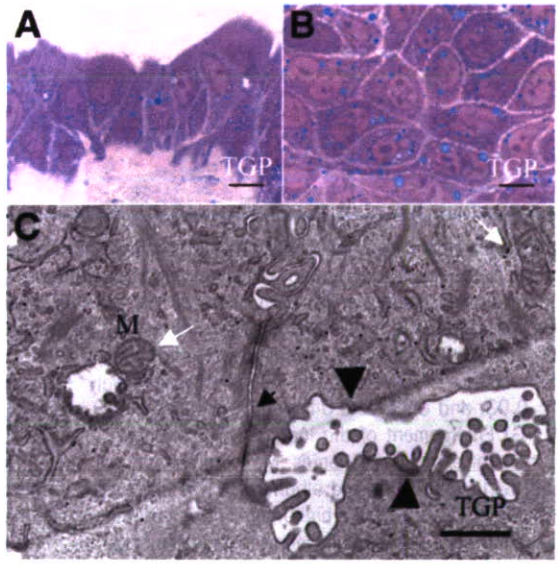

Fig. 5. Perpendicular (A) and horizontal sections (B) of the cultured cells covered with TGP at day 35 (toluidine-blue staining). Hepatocyte-like cells are seen. The size of the cells is between BEC and MH. Scale bars, 10 μm. Ultrastructure of the hepatocyte-like cells at day 35 (C). BC with many microvilli (arrowhead) is shown, and the cytoplasm is rich in organelles such as mitochondria (white arrows) and rough endoplasmic reticulum. A tight junction (an arrow) is observed. Scale bar, 1 μm. TGF, thermoreversible gelation polymer; BEC, bile epithelial cell; MH, mature hepatocyte.

HNF4, which were expressed from the initial day of their appearance, although proteins expressed in cholangiocytes and immature hepatocytes were also co-expressed. The features of the cells were initially very similar to terminal BECs. However, the cells gradually became larger after the injury, and the morphological appearance became similar to that of hepatocytes. The morphological alteration of typical cells was observed in the tips of tubular structures at approximately POD 9. The cellular size was intermediate between typical BECs and MHs. In addition, the hepatocyte-like cells increased in the area where the morphological changes of the cells were observed, such as the area surrounding the ductules. The hepatocyte-like cells could produce glycogen in their cytoplasm, and PAS-positive basement membrane around the cells also disappeared. Conversely, they lost the expression of the marker proteins of BECs and immature cells such as CK19, c-Kit, Thy1, and AFP. The cells with hepatobiliary characteristics seemed to differentiate into MHs. With the reduction of the injured area, hepatocyte-like cells rapidly increased, and most of the injured area was occupied by those cells. These results suggest that the cells induced are quite similar to the ductular hepatocytes that were previously reported. The cells have sometimes been observed after massive (or submassive) hepatic necrosis in rats [3,6,16] and in humans.[17-19] Ductular hepatocytes are considered to be an intermediate form between BECs and MHs, resembling ductal plate cells in the developing human liver. They are located at the periphery of the portal tract, proliferate, and express cholangiocyte and hepatocyte markers. However, it has never clearly been shown that ductular hepatocytes can differentiate into and replace ductules with hepatocytes. Fujita et al.[19] demonstrated by sequential liver biopsies over a period of 14 months that a patient who received an auxiliary partial orthotopic liver transplant after suffering massive necrosis had complete regeneration of natural liver.[19] Therefore, we tried to isolate and culture the intermediate cells from ductular reactions induced by TGP. In addition, we examined whether the cells could differentiate into MHs. In this study, isolated cells co-expressing hepatobiliary cell markers could be purified and cultured for a prolonged period. Although many cell aggregates detached from the dish, some survived and expanded after TGP treatment. The overlay of TGP may prevent detachment and stimulate the expansion of the cultured cells. Histological examinations of the TGP-treated rat livers showed that only the BECs close to TGP could extend processes and differentiate into hepatocytes. The ductules far from TGP never showed ductular reactions. In the current experiment, we isolated the cells in ductules from enucleated liver specimens, which included a large area of the margin (10 mm diameter). The margin may have included non-activated BECs, which TGP might not strongly influence. Such non-activated BECs seemed to decrease. The overlay of TGP may stimulate the selective expansion of the cells influenced by TGP.

Oval cells, which are hepatic progenitor cells, are related to terminal biliary ductules and the so-called canals of Hering.[5,20] They are small cells that have an oval-shaped nucleus and scant cytoplasm containing few organelles.[20,21] The oval cells forming ductular structures are usually surrounded by a continuous basement membrane like BECs. Furthermore, they express phenotypic markers of both immature hepatocytes (AFP) and cholangiocytes (CK7, 8, 18, 19, OV6, GGT).[3-5,20,21] In addition, oval cells are known to express hematopoietic stem cell markers such as c-Kit, Thy-1, and CD34.[4,5] In the current experiment, cells in ductular reactions induced by TGP had a round nucleus and relatively large cytoplasm compared with that of oval cells. Although the cells in the ductules immunohistochemically showed expression patterns of AFP, c-Kit, Thy1, and CK19 similar to those of oval cells, they also expressed hepatic markers such as albumin, transferrin, CYP1A1, and HNF4. These genes were not expressed in the oval cells. In addition, oval cells usually appear when hepatic regeneration is impeded by hepatic toxins or the liver is severely damaged. In this study, only a small part of the liver was injured in normal adult rats, and most hepatocytes were intact, as no toxin was systemically administered. These results clearly suggest that the cells induced by TGP are different from oval cells.

Metaplasia of neighboring hepatocytes (ductular metaplasia) into BECs may occur as a result of TGP treatment. In the current experiment, the existence of ductular reactions in the lesion might have been coincident with the suggestive locations of the portal area, which may have existed before the injury. In addition, before the appearance of the ductular reactions at POD 3, although many dead and injured hepatocytes were observed in the area adjacent to TGP, neither a single nor clustered $CK19^+$-cells were randomly detected in those areas. Conversely, at the time of the initial appearance of the cells in ductular reactions, the size and the features of the nuclei were similar to those of BECs.

Thus, TGP itself may have an effect on certain cells to induce differentiation. Recently, it was reported that TGP might have an effect on the renal differentiation of human bone marrow mesenchymal stem cells.[22] Although there is no direct evidence that TGP can play a key role in stem cell differentiation, TGP treatment may directly or indirectly switch on the signal for hepatic differentiation of stem cells in terminal bile ducts or the canal of

Hering. Thus, further investigation is necessary to clarify the molecular mechanism of hepatic differentiation by TGP.

Acknowledgment: We are grateful to Dr. Atsushi Miyajima (Tokyo University, Tokyo, Japan) and Drs. Yuichi Mori, Hiroshi Yoshioka, and Hideo Sakamaki (Waseda University, Tokyo, Japan) for the generous gifts of the rabbit anti-CK19 antibody and TGP, respectively. We also thank Dr. Yoichi Mochizuki for assistance with TEM and Minako Kuwano, Shigeko Ohnuma, Akiko Hosoyama, Erika Takada, Hiroshi Kohara, Izuru Yokomi, and Tsuneo Igarashi for their technical assistance. We also thank Kim Barrymore for help with the manuscript.

References

1. Nagaya M, Kubota S, Suzuki N, Tadokoro M, Akashi K. Evaluation of thermoreversible gelation polymer for regeneration of focal liver injury. Eur Surg Res 2004;36:95-103.
2. Yoshioka H, Mikami M, Mori Y, Tsuchida E: A synthetic hydrogel with thermoreversible gelation: preparation and rheological properties. J Macromol Sci 1994;A31:113-120
3. Sell S. The role of progenitor cells in repair of liver injury and in liver transplantation. Wound Repair Regen 2001;9:467-482.
4. Fausto N, Liver regeneration and repair: hepatocytes, progenitor cells, and stem cells. HEPATOLOGY 2004;39:1477-1487.
5. Alison MR, Vig P, Russo F, Bigger BW, Amofah E, Themis M, et al. Hepatic stem cells: from inside and outside the liver? Cell Prolif 2004;37:1-21.
6. Sirica AE, Williams TW. Appearance of ductular hepatocytes in rat liver after bile duct ligation and subsequent zone 3 necrosis by carbon tetrachloride. Am J Pathol 1992;140:129-136.
7. Wagers AJ, Sherwood RI, Christensen JL, Weissman IL. Little evidence for developmental plasticity of adult hematopoietic stem cells. Science 2002; 297:2256-2259.
8. Tsanadis G, Kotoulas O, Lollis D. Hepatocyte-like cells in the pancreatic islets: study of the human foetal pancreas and experimental models. Histol Histopathol 1995;10:1-10.
9. Mitaka T, Sato F, Mizuguchi T, Yokono T, Mochizuki Y. Reconstruction of hepatic organoid by rat small hepatocytes and hepatic nonparenchymal cells. HEPATOLOGY 1999;29:111-125.
10. Yang L, Li S, Hatch H, Ahrens K, Cornelius JG, Petersen BE, et al. In vitro trans-differentiation of adult hepatic stem cells into pancreatic endocrine hormone-producing cells. Proc Natl Acad Sci U S A 2002; 99:8078-8083.
11. Miura K, Nagai H, Ueno Y, Goto T, Mikami K, Nakane K, et al. Epimorphin is involved in differentiation of rat hepatic stem-like cells through cell-cell contact. Biochem Biophys Res Commun 2003;311:415-423.
12. Bucher NL. Regeneration of mammalian liver. Int Rev Cytol 1963;15: 245-300.
13. Desmet V, Roskams T, Van Eyken P: Ductular reaction in the liver. Pathol Res Pract 1995;191:513-524.
14. Popper H. The relation of mesenchymal cell products to hepatic epithelial system. In: Popper H, Schaffner F, eds. Progress in Liver Diseases. Philadelphia: W.B. Saunders, 1990:27-38.
15. Michalopoulos GK, Barua L, Bowen WC. Transdifferentiation of rat hepatocytes into biliary cells after bile duct ligation and toxic biliary injury. HEPATOLOGY 2005;41:535-544.
16. Sirica AE. Ductular hepatocytes. Histol Histopathol 1995;10:433-456.
17. Roskams T, De Vos R, Van Eyken P, Myazaki H, Van Damme B, Desmet V. Hepatic OV-6 expression in human liver disease and rat experiments: evidence for hepatic progenitor cells in man. J Hepatol 1998;29:455-463.
18. Haque S, Haruna Y, Saito K, Nalesnik MA, Atillasoy E, Thung SN, et al. Identification of bipotential progenitor cells in human liver regeneration. Lab Invest 1996;75:699-705.
19. Fujita M, Furukawa H, Hattori M, Todo S, Ishida Y, Nagashima K. Sequential observation of liver cell regeneration after massive hepatic necrosis in auxiliary partial orthotopic liver transplantation. Mod Pathol 2000;13:152-157.
20. Paku S, Nagy P, Kopper L, Thorgeirsson SS. 2-Acetylaminofluorene dose-dependent differentiation of rat oval cells into hepatocytes: confocal and electron microscopic studies. HEPATOLOGY 2004;39:1353-1361.
21. Hixson DC, Faris RA, Thompson NL. An antigenic portrait of the liver during carcinogenesis. Pathobiology 1990;58:65-77.
22. Hishikawa K, Miura S, Marumo T, Yoshioka H, Mori Y, Takato T, et al. Gene expression profile of human mesenchymal stem cells during osteogenesis in three-dimensional thermoreversible gelation polymer. Biochem Biophys Res Commun 2004;317:1103-1107.

ELSEVIER

Journal of Hepatology 45 (2006) 90–98

Journal of Hepatology

www.elsevier.com/locate/jhep

Expression of CD44 in rat hepatic progenitor cells

Junko Kon, Hidekazu Ooe, Hideki Oshima, Yamato Kikkawa, Toshihiro Mitaka*

Department of Pathophysiology, Cancer Research Institute, Sapporo Medical University School of Medicine, South-1, West-17, Chuo-Ku, Sapporo 060-8556, Japan

See Editorial, pages 1–4

***Background/Aims*: Small hepatocytes (SHs) are hepatic progenitor cells, but the phenotypical difference between SHs and mature hepatocytes (MHs) has never been demonstrated.**

***Methods*: The profile of gene expression was examined to clarify the difference between SHs and MHs by using a DNA microarray. Genes that were specifically expressed in SHs were identified and RT-PCR analysis of them was performed. Immunocytochemistry for CD44 standard form (CD44s) and variant form 6 (CD44v6) was performed using cultured SHs and the D-galactosamine (GalN)-injured rat liver. From the GalN-treated liver, CD44s $^{+}$ cells were obtained by sorting and RT-PCR analysis was performed.**

***Results*: Analysis using the DNA microarray and RT-PCR of them revealed restricted expression of CD44s and CD44v6 in SHs. In culture, CD44s appeared at day 3 and increased with the proliferation of SHs. CD44v6 expression was delayed compared to that of CD44s. With GalN-administration, CD44 $^{+}$ hepatocytes appeared around periportal areas at days 3 and 4 and then decreased. Sorted CD44s $^{+}$ cells could form colonies and possessed hepatic markers.**

***Conclusions*: CD44 is a specific marker of SHs. The expression of CD44 mRNA and protein is restricted to SHs, and is up-regulated at the time when SHs start to proliferate both in vitro and in vivo.**

***Keywords*: CD44s; CD44v6; Small hepatocytes; Proliferation; Maturation**

1. Introduction

Small hepatocytes (SHs) are a subpopulation of hepatocytes that have high growth potential in culture [1–4]. The cells are less than half the size of mature hepatocytes (MHs), but they possess hepatic characteristics [5,6]. SHs can clonally proliferate to form colonies that survive for more than 5 months in defined medium [5,6] and can differentiate into MHs by interacting with hepatic nonparenchymal cells (NPCs) [7] or as a result of treatment with Engelbreth–Holm–Swarm gel [8]. Thus, we consider that SHs may be 'committed progenitor cells' that can further differentiate into MHs. Although SHs are primary cells that are freshly prepared from rat liver, they can also proliferate after cryopreservation [9].

The molecular mechanisms regulating the characteristics of SHs remain to be elucidated. In addition, their precise origin and location within the liver are not clear because the preparation of purified SHs is difficult and specific markers for SHs have never been identified. Therefore, it is important to identify specific genes and proteins expressed in SHs, especially cell membrane-integrated proteins, because it will be possible to clarify the characteristics of the cells by the methods of cell sorting.

Received 18 May 2005; received in revised form 10 January 2006; accepted 17 January 2006; available online 28 February 2006

* Corresponding author. Tel.: +81 11 611 2111x2390; fax: +81 11 615 3099.

E-mail address: tmitaka@sapmed.ac.jp (T. Mitaka).

Abbreviations:: BECs, biliary epithelial cells; CD44s, CD44 standard form; CD44v, CD44 variant form; C/EBPα, CCAAT/enhancer binding protein α; CYP, cytochrome P450; GalN, D-galactosamine; HA, hyaluronic acid; LECs, liver epithelial cells; MH, mature hepatocyte; NPC, hepatic nonparenchymal cell; SH, small hepatocyte.

0168-8278/$32.00
doi:10.1016/j.jhep.2006.01.029

The CD44 gene encodes for a family of alternatively spliced, multifunctional adhesion molecules that participate in lymphocyte–endothelial cell interactions as lymphocyte homing receptors [10–12], and in adhesion of cells to extracellular matrix [13], T cell activation and adherence [14], and metastasis formation [15]. CD44 standard form (CD44s) is composed of a short cytoplasmic tail, a transmembrane region and two extracellular domains. There are 10 additional exons (v1–v10). Although the expression of CD44 variant forms (CD44v) was initially considered to occur as a result of aberrant splicing in tumor cells, variant expression was subsequently detected in normal cells [16]. The expression of variant forms in hematopoietic cells has been reported [17–19].

In the present study, we found that both CD44s and CD44v6 were expressed in cultured SHs and their expression decreased with the maturation of the cells. Although biliary epithelial cells (BECs) also expressed CD44s, no other epithelial cells within the normal rat liver did. However, when the rat liver was severely injured by D-galactosamine (GalN) treatment, CD44s$^+$ epithelial cells appeared near Glisson's capsule in the liver lobules and, by using a specific antibody, the cells could sorted and thereafter cultured. These CD44s$^+$ cells expressed hepatic marker genes and could proliferate to form colonies consisting of SHs.

2. Materials and methods

2.1. Isolation and culture of SHs

Male F344 rats (Sankyo Lab Service Corporation, Inc., Tokyo, Japan) weighing 150–200 g were used to isolate hepatic cells by the two-step liver perfusion method of Seglen [20] with some modifications [2]. Briefly, suspensions of liver cells were centrifuged at 50×*g* for 1 min. The supernatant was used to prepare SHs and the precipitate was used to prepare MHs. The details of the isolation and culture procedure were previously reported [7]. After the number of viable cells was counted, cells were plated on dishes (7.5×10^4 cells/35-mm, 10×10^5 cells/100-mm dish; Corning Glass Works, Corning, NY). SH colonies cultured in a 100-mm dish were collected at day 14 and cryopreserved at −80 °C. The details of the method were previously reported [9]. After cryopreservation, SHs were thawed and suspended in the culture medium. To induce the maturation of SHs, they were overlaid with growth factor-reduced Matrigel® (BD Biosciences, Bedford, MA) at day 14 after thawing and the cells were then cultured. The details of the method were previously reported [8].

2.2. DNA microarray

Differences of the expression profiles of SHs and MHs were analyzed using a microarray approach. A DNA microarray spotted with 14,815 cDNAs (Agilent rat cDNA microarray kit) was purchased from Agilent Technologies, Inc. (Palo Alto, CA). Poly(A)$^+$ RNAs were prepared using ISOGEN (Nippon Gene, Tokyo, Japan) and mRNAs were prepared using a GenElute™-mRNA miniprep kit (Sigma Chem Co, St Louis, MO). Prepared mRNAs were labeled with Cy5- and Cy3-dUTP by reverse transcription. Analysis of the microarray was performed by Hokkaido System Science (Sapporo, Japan).

2.3. RT-PCR

Total RNA was isolated using ISOGEN. Reverse transcription and PCR amplification (RT-PCR) were performed in a one-step reaction according to the manufacturer's instructions (Invitrogen, San Diego, CA). Sequences of forward and reverse primers used are listed in Table 1. The constitutively expressed gene glycerol 3-phosphate dehydrogenase (GPDH) was also reverse-transcribed in a separate reaction as a qualitative and quantitative control.

2.4. Northern blot analysis

Northern blot analysis was performed as previously reported [21]. Probe labeling and RNA detection were performed according to the manufacturer's instructions for the AlkPhos Direct Labelling and Detection System with CDP-Star (Amersham Biosciences, Piscataway, NJ). For probes, the full-length CD44s and partial 450 bp GPDH fragment were used.

2.5. Western blot analysis

After washing with PBS twice, the cells were dissolved in lysis solution (20 mM Tris–HCl [pH 7.4], 150 mM NaCl, 2.5 mM EDTA, 1% Triton-X100, 1% aprotinin, and 20 mg/ml leupeptin). The cells were kept on ice for 30 min and sonicated. After the sonication, the solution was centrifuged at 22,000×*g* for 20 min. The supernatant was kept at −80 °C until use and the protein content was measured using a BCA assay kit (Pierce, Rockford, IL). Western blot analysis was carried out as previously described [7].

2.6. Immunostaining

Antibodies used for immunostaining are listed in Table 2. SHs in a 35-mm dish were used for immunocytochemistry. After washing with PBS, the cells were fixed in 70% cold ethanol. After blocking with BlockAce (Dainippon Pharmaceuticals Co., Osaka, Japan) for 30 min at RT, cells were incubated with the primary antibody for 60 min at RT. Dishes were rinsed with PBS and subsequently incubated with an Alexa^{488}-conjugated antibody (Molecular Probe, Eugene, OR) for 30 min at RT. In case of double staining, the secondary antibody was applied for 60 min. After washing with PBS, the Alexa^{594}-conjugated antibody (Molecular Probe) was applied for 30 min. Finally, cells were embedded with 90% glycerol including 0.01% *p*-phenylenediamine and 4,6-diamidino-2-phenylindole (DAPI).

For immunohistochemistry, the liver was frozen at −80 °C until use. Then 7-μm-thick sections were prepared and air-dried. The staining procedure used for the sections was the same as for immunocytochemistry. A confocal laser microscope (Zeiss, Jena, Germany) was used for observation.

2.7. D-galactosamine administration

GalN (Sigma; 75 mg/100 g body weight dissolved in PBS) was intraperitoneally given to male F344 rats weighing 150–200 g [22]. The animals were killed 1–5 days after the treatment and their livers were removed. Liver slices were prepared, immediately frozen in liquid nitrogen and kept at −80 °C until use.

2.8. Cell sorting and culture

Four days after GalN treatment, hepatic cells were isolated as described above. The isolated cells were centrifuged at 50×*g* for 1 min. The supernatant was collected and then centrifuged again. After the same procedure was repeated, the supernatant was centrifuged at 150×*g* for 5 min and the pellet was suspended in PBS containing 2 mM EDTA and 0.5% BSA. An anti-CD44 antibody (625 ng/ml) was added and, following incubation for 10 min, cells were washed